International Journal of Emerging Technology and Advanced Engineering
Website: www.ijetae.com (E-ISSN 2250-2459, Scopus Indexed, ISO 9001:2008 Certified Journal, Volume 12, Issue 07, July 2022)
Manuscript Received: 18 May2022, Received in Revised form: 26 June 2022, Accepted: 02 July 2022 DOI: 10.46338/ijetae0722_18

Membrane Backwash Performance Improvement-A Review

M. J. Mopeli[1], P. B. Sob[2], A. A. Alugongo[3], T. B. Tengen[4]
[1,2,3,4]*Department of Industrial Engineering & Operations Management and Mechanical Engineering, Faculty of Engineering and Technology, Vaal University of Technology, Vanderbijlpark 1900, Private Bag X021, South Africa*

***Abstract* -To date, different models and parameters have been used to design membrane backwash system for different applications and in most cases this has led to improved performance of membrane system. However, some of these developed backwashing system are inefficient, due to poor modelling of relevant physical parameters and variables that affect backwash system. An efficient cleaning design of a membrane backwash system has proven to be a promising approach or technique in improving membrane performance for different applications. As such, it is important to study all the relevant models and parameters that can be used in designing a membrane backwash system to improve the overall performance of the membrane system for oil-water separation application. In this review study, a series of models are identified and their potential application to establish critical operating process during backwash. This report has three section, namely: Identification of critical backwash operating conditions that could potentially optimize backwash system, flux recovery models and lastly, fouling-based models. The purpose of this review is to identify relevant parameters and relevant models during backwash process. More consideration is based on demonstrating the effectiveness of high intensity of critical operating condition during backwash, which canforce the oil droplet blockage to be dislodged out of the membrane pores with ease. As result, reduction in backwash duration and improve the overall performance. This study concludes as follows; the identification of critical parameter, majority of the models are based on conservation principle which is a (collective of conservation mass, momentum and energy) governed by Navier-Stokes laws. Also, modelling the oil droplet dislodging phenomenon, much consideration should be based on the driving back-pressure and interfacial tension forces, to deform and push the oil droplet blockage out of the pores. Furthermore, developed critical pressure models on filtration phase do not directly consider the different fouling formation between oil and solid particles**.

***Keywords* - backwash; fouling; modelling; critical operating condition; flux recovery**

I. INTRODUCTION

The significant increase of industrial oil waste such as: Oil spills, oily water discharge and oil leakage have become the most critical concern for environmental degradation[2].

As result, two-thirds of the global population will inevitable be living in water-stressed regions in the near future[2]. Due to water pollution, deaths and illnesses have significantly increased worldwide [2]. The demand for advanced water purification technology has increased the overall market for membrane technology to be implemented on an industrial scale, this is due to their significant advantage when compared to numerous conventional filtration techniques [3]. Membrane technology holds great potential in oil/water separation application but the persisting fouling problem affects membrane performance[3]. Numerous studies on membrane backwash have been conducted with the aim to reduce the fouling effect on membrane technology [4, 5]

Since (1990 – 2018) several backwashing or backpulsing publications usedin MF / UF processes have been reported, the total number of publications focusing only on backwashing was estimated to be 1056 and backpulse has an estimated value of 110 publications till 2018. The following data was collected fromhttp://apps.webofknowledge.com in January 2019 by Gao et al. [6]. This includes the three backwashing review studies which were published, in 2016, 2017 and 2018 respectively and one backpulse review by Gao et al. (2019) [6]. The 2016report reviews backwashing as cleaning technique to control fouling in wastewater treatment for membrane bioreactors [7]. The 2017 review focuses on low-pressure membranes backwash for drinking water treatment [8]. Lastly, 2018reviews fouling detection and mitigating techniques from a process control perspective by use of models[4].However, none of the reviews has identified relevant models and parameters to improve backwash performance which are address in this review study, different subject including backwash performance in various applications such as: operating parameter optimization, as well as flux prediction modelling and mechanism analysis studies are covered in this review study.

Membrane cleaning can be classified into two categories namely: physical and chemical method. For physical, it incorporates process such as: pneumatic, hydraulic, mechanic, and electric application[9].

International Journal of Emerging Technology and Advanced Engineering
Website: www.ijetae.com (E-ISSN 2250-2459, Scopus Indexed, ISO 9001:2008 Certified Journal, Volume 12, Issue 07, July 2022)

While chemical cleaning usually incorporate chemical solution such as: acids, oxidants, surfactants and bases[9]. While some researchers resorted to chemical clean as means to eliminate the irreversible foulant layer [10]. The main drawback of chemical cleaning is that it impairs membrane selectivity, as result, shortens membrane lifespan.Since the aim of the study is to improve the performance of a membrane backwash system for efficient wettability process, the following section will only outline a brief summary on physical cleaning techniques based on hydraulic application.

The hydraulic cleaning incorporate process such as: forward flushing, backwashing or backpulsing which is the most common cleaning technique for fouling removal[9]. The periodic reverse flow is capable of dislodging and lift-off oil droplets (foulants) from the membrane pores and surface respectively. As result, preventing fouling elevation from reversible to irreversible by minimizing concentration polarization effect[11]. The forward flush is performed during filtration phase commonly by application crossflow to improve the shear effect on membrane surface[9]. Backpulsing (back-shock) is high magnitude and rapid type of backwash. It's short duration (<1s) and high intensity application has been proven to be effective to remove non-adhesive foulants on the membrane surface[12]. However the intensive backwash application even though proven to be effective to mitigate fouling, it has not been given considerable amount of attention in both modelling and experimentation studies[13]. Any improvement to the backwashing technique has huge potential to improve the overall performance, cost-effectiveness of both current and future membrane technology [14, 15].

Three factors differentiating backpulse from backwash: Firstly, unlike backwash, backpulsing is a kind of reverse flow cleaning procedure that induce transmembrane pressure (TMP) for a significant short period. (usually less than 1 s) and is usually used in conjunction with cross-flow velocity (CFV) at corresponding high amplitude [6].Secondly, thesignificant difference between backpulse and backwash is the utilized amplitude (speed and force). Backpulse is generally characterized by a high frequency and short duration [6]. While backwash is usually performed for a few minutes for a selected time interval ranging from minutes or longer. However, backpulse only last for a fraction of seconds in every few seconds [6].Lastly, for backwash process to be performed the filtration phase needs to be stopped temporary which interrupts the production [6]. On the contrary, backpulse application introduce no interrupts to the filtration phase.

Despite the difference in procedure during operation between backwash and backpulse. However, their principle of operation is more or less the same, as they utilize the reverse flow phenomenon to clean or dislodge foulants found on the membrane structure. The aim is merge both backpulse and backwash operating procedure to improve the cleaning efficiency by utilizing high amplitude reverse pressure and reducing backwash duration.

1.2 Backwash fundamentals

Backwashing is one of the most commonly applied procedure for cleaning membrane surface, whereby the flow direction is reversed to dislodge membrane accumulated contaminates, this procedure may prevent the transition of reversible to irreversible fouling [16-18]. The best operating parameters that gave best performance during backwash need to be identified and modelled based on preliminary evaluation test of the dynamic relationship between effective backwash parameters. This evolving modelling approach in membrane technology has attracted a lot of attention to many researchers to advance membrane processes[19]. To explore this evolving approach, some of the important aspects to be considered in this modelling identification review: Understanding membrane fouling and subsequent permeate flux recovery model which are associated with optimizing membrane backwash system for stable and efficient wettability process. This report divided into three section, namely: firstly, identification of critical backwash operating conditions that could potentially optimize backwash system. Secondly, flux recovery models and lastly, fouling-based models.

Like backpulse: amplitude, duration and frequency are three fundamental parameters associated with effective backwash. These fundamental parameters should be optimized to improve backwash performance [6]. The reverse applied pressure value defines the amplitude, while frequency is define as the time interval between two consecutive pulses, lastly the duration is the time taken by each pulse [12, 20]. Backwash may successfully eliminate hydraulically reversible fouling and reducing polarization concentration if the fundamental operating conditions are satisfied [6]. The external fouling and non-adhesive fouling are typical hydraulically reversible fouling removed by backwash. These external and internal fouling are categorized by the factors associated with fouling formation as demonstrated in section A [21]. Cake layer accumulation is generally identified as an external fouling, while internal fouling is induced by pore blockage or constriction.

International Journal of Emerging Technology and Advanced Engineering
Website: www.ijetae.com (E-ISSN 2250-2459, Scopus Indexed, ISO 9001:2008 Certified Journal, Volume 12, Issue 07, July 2022)

One the other hand non-adhesive and adhesive fouling are defined based on the types of feed concentration[22]. Non-adhesive fouling is generally suspended particles and inorganic fouling, while biofouling, colloidal and organic fouling is typically adhesive fouling [23].

1.3 Evaluating backwash efficiency

This experimentation for validation study evaluates the optimal operating conditions of backwash through predetermined modelling approach. Not only does the optimized backwash procedure results in efficient performance during filtration due to high permeation flux recovery but also results in reduced operating cost which is beneficiary for long-term operation. Poor backwash results to inadequate cleaning procedure of membrane. This is due to poor driving backwash-pressure that is less than the required critical back-pressure to effectively dislodge contaminates results in inefficient cleaning. The schematic diagram below illustrate an inefficient backwash process in figure 1.1 below[6].

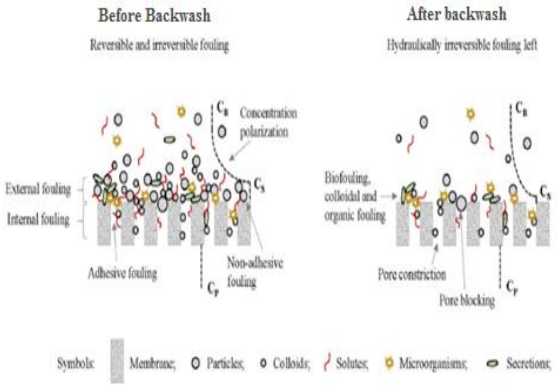

Fig1.1 Schematic illustration of inefficient backwash process. Adapted from Ref.[6].

As illustrated by the schematic diagram above: before backwash, the solute diffusion rate by large particle accumulation and the solute concentration on the membrane surface are far greater than the bulk solute concertation. As a result, solvents experience decline in permeation flux due to an increase in osmotic pressure by concentration polarization which offset the TMP during filtration [24].Applying high amplitudebackwash, the accumulated foulants on the membrane surface can all be removed with ease. Consequently,improving backwash cleaning efficiencyand reducing cost by shortening operation duration [6].

Backwash efficiency can be evaluated by considering the followingaspects of performance. One being permeation rate evaluation such as: flux, transmembrane pressure (TMP) and membrane resistance and permeability monitoring. The other being the production quality monitoring which entails: measuring the net permeate volume and quality after a certain filtration phase. The backwash evaluation strategies are summarized by [8] and[6] backwash and backpulse review studies respectively.In summary, inadequate backwash process leads to accumulation of foulant particle on the membrane which consequently becomes increasingly difficult to remove during the backwash cycle. Due totransition effect of the foulant layer built-up, from reversible to irreversible causing significant problems over the extended operating duration of the membrane system [25].

1.4 Factors affecting backwash effectiveness

Feed properties, operating parameters and membrane properties are the main factors that have influence on backwash efficiency [4, 6].

1.4.1 Feed properties

Firstly, the influence of backwash on the mitigation of fouling on the membrane surface depends highly on the types of foulants, which is predominantly dictated by the composition of the feeding solution [6]. Secondly, the rapid foulant accumulation on the membrane surface and rapid flux decline directly proportional to amount of feed concentration [26]. Consequently, backwash is reported to be less effective on solution with high concentration [27].Membrane fouling arising from oily organic matter remains one of the greatest challenges in the treatment of oily wastewater[28]. This is because oils are highly susceptible to adsorption onto the membranes, which leads to blocking of the pores, causing the rapid decline of the flux and separation efficiency. In general, oily wastewater streams contains oils in different forms, including : stable emulsified oils, unstable dispersed oils and free-floating oils (spilled oils on the ocean). The dispersed oils have a strong tendency to coalesce and spontaneously evolve into free-floating oils. However, unlike free-floating oils, dispersed oils are randomly distributed in water. In contrast, emulsified oils are rather stable due to the presence of molecules acting as surfactants.

1.4.2 Membrane properties

Membrane material have a huge influence on application of backwash in fouling mitigation [6].

International Journal of Emerging Technology and Advanced Engineering
Website: www.ijetae.com (E-ISSN 2250-2459, Scopus Indexed, ISO 9001:2008 Certified Journal, Volume 12, Issue 07, July 2022)

Unlike polymeric membrane which are more sensitive, ceramic membrane are known to be more sustainable to harsh operating condition such as (high pressure, chemical cleaning and temperature) [29].Based on the membrane properties, the filtration process uses two separation methods, one being size exclusion (i.e. sieving) effect and the other being selective wettability [30]. The first effect means the membrane allows water to permeate through the membrane under an applied pressure while restricting oil droplets that are larger than pores of the membrane[28]. The second effect ensures that the oil droplets do not wet and permeate the membrane through its selective wetting properties (e.g., hydrophilicity and oleophobicity underwater) [28]. Membrane property fatigueanalyses should be conducted during material selection process as recommended by most researchers [6].

1.4.3 Membrane surface properties

Surface properties such as hydrophilicity/hydrophobic and surface charge are also the contributing factors in membrane fouling formation [6]. Several studies that investigated the surface properties effect, have all reached the same conclusion that properties are indirectly affecting the backwash efficiency [6]. To date, the main reason for membrane surface property advancement (surface modification of membrane) is to improve membrane hydrophilicitywhich improves the membrane performance. To also mitigate the fouling and optimize the hydrodynamic conditions of the membrane, different membrane techniques have been experimented. The hydrophobic membranes are modified to be strong hydrophilic membranes by (blending, coating and grafting) some of the inorganic nanoparticles such as Al_3O_4, SiO_2, Fe_3O_4, ZrO_2, and TiO_2 onto the membrane surface. It is generally agreed that by using highly hydrophilic membranes, the adhesion of oil on the membrane surface could be decreased which, subsequently, results in the reduction of membrane fouling and enhancement of water productivity[31]. In summary, oily wastewater filter membranes with super-hydrophilicity and underwater super-oleophobicity can effectively decrease membrane fouling during separation of oil-in-water emulsions[32].

1.4.4 Membrane pore size

The fouling formation and membrane pore size have a very close relationship [33]. For example if the foulants size is slightly smaller or the same size as the membrane pore, pore blockage is more likely to be the most dominate type of fouling formation [6].

However if the foulants are larger the pore size, external fouling or cake layer formation will be the dominate fouling formation [6]. Therefore membrane pore size was report to have influence on backpulse efficiency [34]. Membrane technology methods of separation in pressure-driven processes categorized by pore size include: microfiltration (MF), ultrafiltration (UF), Nano-filtration (NF) and reverse osmosis (RO)[10, 28].Traditional ultrafiltration and microfiltration membranes applied for separating oily wastewater mainly take advantage of the 'size-sieving' effect driven by applied pressure, in which oil droplets with certain sizes are not allowed to pass through the 'pores' of the membrane[28].

1.4.5 Operation parameters

The critical operating conditions are required for effective backwash procedure. The amplitude (reverse-pressure) is a prerequisite to the optimizing the backwash process [6]. However, it was discovered that very intense backpulse/backwash can break foulants with very fragile structures (foulants transported back to the feed), which will emulsify the feed solution and as a result make it more difficult to separate [6]. Operating parameters such as backwash pressure, backwash flow and backwash strength (i.e., ratio between backwash and filtration flux) have also been discussed in previous studies [5]. The critical reverse pressure of a minimum (60 – 85 kPa) was disclose as prerequisite parameters for optimal operating condition in dead-end Microfiltration (MF) process by [35]. For polymeric membrane which are less sustainable to harsh conditions, the highest limit of the applied reverse pressure during backwashor backpulse is an important concern [6].In summary, it would be interesting, as a perspective, to study the backwash parameters effect on the energy consumption and thus develop an optimal backwashing strategy that would maximize the net water production while minimizing the fouling effect[5].

1.4.6 Frequency and duration

The effect of both frequency and duration on backwash efficiency vary from application to application [6]. Their influence depend on the type of fouling formation and fouling mitigating procedure used [6].[36] developed a model to predict optimal duration and frequency of a backwashprocedure, to conclude their finding, they declare that it is more important to choose an acceptable duration than a proper frequency [6]. Several other researchers have demonstrated the importance of controlling the backwash interval (BWI) and backwash duration (BWD)[5].

International Journal of Emerging Technology and Advanced Engineering
Website: www.ijetae.com (E-ISSN 2250-2459, Scopus Indexed, ISO 9001:2008 Certified Journal, Volume 12, Issue 07, July 2022)

They all agree, that prolonged filtration duration would decrease the product water due to a more pronounced irreversible fouling [4, 5]. On the other hand, short backwash interval (~20 min) can lead to frequent backwash which decreases the net water production [4]. Moreover, increasing backwash duration can lead to higher product flow (i.e., less fouling) but higher water consumption [4]. It was discovered that backwash interval has the most significant effect on the specific flux reduction and net water production. The effects of backwash duration and backwash flow are more important on Net Water Production[5].

1.4.7 Summary

The influence of each individual parameters on backwash efficiency has been addressed by several studies in attempt to optimize the backwash procedure [4-6]. It is clear that for a given system, depending on the type of application, there exist a critical value for each parameters. Not only do the models help identify this critical value to predict the productivity of the membrane, but also provide a framework to assess the backwash efficiency in fouling mitigation [6]. In addition these parameters are connected to each other and their dynamic relationship should always be considered during modelling and experimental studies. The influence of filtration parameters such as TMP, permeate flux and CFV on efficiency of backwash is also important and should be considered [6].

Section A

II. Identifying Critical Backwash Operating Conditions

This section is further subdivided into two sub-sections. Sub-section one: identifies relevant models on backwash. While, sub-section two: outlines experimental studies to validate the effectiveness critical operating conditions.

2.1 Sub-section one

There are several approaches to address backwash modelling. One is to focus on the single foulant behaviour during backwash (Eulerian approach), two is to consider the fouling phenomenon as a continuous process so the mass transfer of the system needs to addressed (Lagrangian approach) [6]. Below are some of the strategic backwash modelling studies based on Fluid dynamics and Navier-Stokes laws.

2.1.1 Model (I)

Model (I) is the analytic model concept based on the Force balance concept as illustrated by the schematic diagramin figure 2.1 below [6]. The force balance concept illustrate the mechanical forces required to dislodge and remove the accumulated foulants on membrane structure during backwash process.

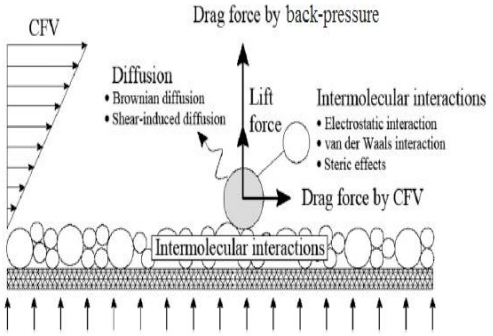

Fig 2.1 illustrates the force balance concept. Adopted from Ref [6]

During forward filtration phase, reversible foulants accumulates on membrane surface. Backwash cleaning efficiency as function of multiple parameters. Identification andmodellingthese parametershelps reduce the number of experimentation require to optimize the backwash process. Theimproved backwash procedure is capable of inducing sufficient shear effect to lift and sweep the reversible foulants from the membrane. The schematic diagram above illustrates the forces acting on the deposited foulant during backwash period, this forces are generally assumed to be caused by the following fluid flow dynamics[6]:

- Hydrodynamics forces namely: drag force by reverse-pressure and corresponding flow velocity. Lastly, the inertial lift force [37, 38];
- Foulants diffusion forces by Brownian diffusion, shear-induced diffusion are the only types considered
- Intermolecular interaction forces resulting into accumulation of foulants caused by either foulant-foulant or foulant-membrane interaction is described by: the electrostatic interaction, van der Waals interaction and steric effects.

Foulants may be lifted and swept off by application of backwash, if the exerted drag force which is associated with inertial lift force and reverse diffusion forces is sufficient to overcome the bonded interaction forces between foulants and the membrane.

Furthermore, high CFV during filtration phase may also reduce the concentration polarization effect if the drag force by CFV is greater than the resistive forces tangential

International Journal of Emerging Technology and Advanced Engineering
Website: www.ijetae.com (E-ISSN 2250-2459, Scopus Indexed, ISO 9001:2008 Certified Journal, Volume 12, Issue 07, July 2022)

to the membrane surface (e.g., forces from intermolecular interactions and diffusion) [6].

2.1.1.2 Discussion and interpretation of results

This analytic model concept initial came about as just a theoretical framework recommended to future researchers in backwash optimizing, it was never mathematical modelled. However,at the later stage[1]Model (V)adopt this theoretical concept and developed a simulation study based in computational fluid dynamic (CFD), under which all the parameter illustrate in the schematic diagram in figure (2.1) were incorporated in the derivation of mathematical model (V) (see page 4 for further details). As such, thesimulation results obtain in model (V) suffice to validate theseanalytic model concept model (I).

2.1.1.3 Conclusion

In summary, the motion of foulants is determined by the combination of all the forces, and thus determines the separation efficiency of backwashing on fouling removal. The acting forces are different for each fouling accumulation. For example, large foulants (larger than 1 μm), backwash is more efficient by use of hydrodynamics forces. On the contrary, for submicron foulant sizes, backwash through foulant diffusion effect on these accumulation foulants is considered to be a more effective approach [39]. Backwash efficiency is reported to depend on the following factors: feed properties, membrane properties and operating parameters. Therefore, these parameters need be considered and introduce in the analytic model by future studies.

2.1.3 Model (II)

To date, most developed models to investigate the critical operating parameter are based on oil droplet deformation and permeation through the membrane during filtration phase [40]. The critical pressure oil droplet deformation effect across an interface of two immiscible fluids was initially modelled by Young-Laplace equation [41]. According to the equation, the critical pressure is product of the interface tension and the mean curvature coefficient as follows [41, 42]:

$$\Delta P = 2\sigma\kappa \qquad (1)$$

Whereby (κ) is the mean curvature coefficient of the interface which is computed by summing two principle curvatures but neglecting the gravitation effect.

The following assumption results in mean curvature of the arbitrary cross section as follows [41]:

$$\kappa = \frac{C_p \cos\theta}{2A_p} \qquad (2)$$

Whereby $\left(A_p\right)$ and (C_p) are cross sectional area and circumference respectively substituting equation (2) in equation (1) the Young-Laplace critical pressure is obtained as follows [41]:

$$P_{cr} = \frac{\sigma C_p \cos\theta}{A_p} \qquad (3)$$

In recent studies, Young-Laplace equation was modified to account for the finite oil droplet size variation. The schematic diagram in figure 2.4below illustrate the deformation of oil droplet at the pore entrance of a membrane[43].

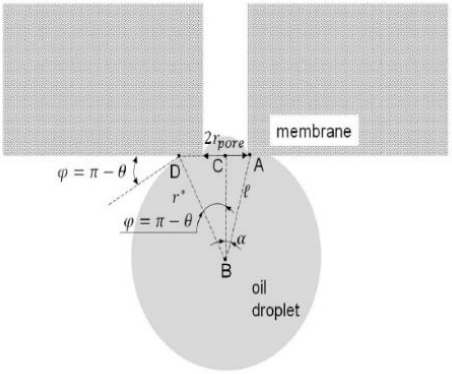

Fig 2.4 Oil droplet deformation and Permeation. Adopted from Ref.[43]

Based on the mathematical approach (trigonometry), the schematic diagram triangle ABC and BCD, computing of the drag force arm (ℓ) around A, the sine droplet angle of repose(α) and the mean curvature $\left(r^*\right)$ were obtained as follows [43, 44]:

$$\ell = \sqrt{r_p^{\,2} + \left[r^* \cos\theta(\pi - \theta)\right]^2} = \sqrt{r_p^{\,2} + \left(r^* \cos\theta\right)^2} \qquad (4)$$

$$\sin\alpha = \frac{1}{\sqrt{1 + \left(\frac{r^*}{r_p}\right)^2 \cos^2\theta}} \qquad (5)$$

International Journal of Emerging Technology and Advanced Engineering
Website: www.ijetae.com (E-ISSN 2250-2459, Scopus Indexed, ISO 9001:2008 Certified Journal, Volume 12, Issue 07, July 2022)

$$r^* = \frac{r_p}{\cos\theta}\left[\frac{4\left(\frac{r_d}{r_p}\right)^3\cos^3\theta+\left(2-3\sin\theta+\sin^3\theta\right)}{2-3\cos\theta+\cos^3\theta}\right]^{\frac{1}{3}} \quad (6)$$

After manipulating and substituting the mean curvature in equation (6) into Young-Laplace critical pressure equation was obtained as follows in equation (7). The modification of Young-Laplace in Equation (7) is derived by Nazzal and Wiesner[41]:

$$P_{cr} = \frac{2\sigma\cos\theta}{r_p}\sqrt[3]{1-\frac{2+3\cos\theta-\cos^3\theta}{4\left(r_d/r_p\right)^3\cos^3\theta-\left(2-3\sin\theta+\sin^3\theta\right)}} \quad (7)$$

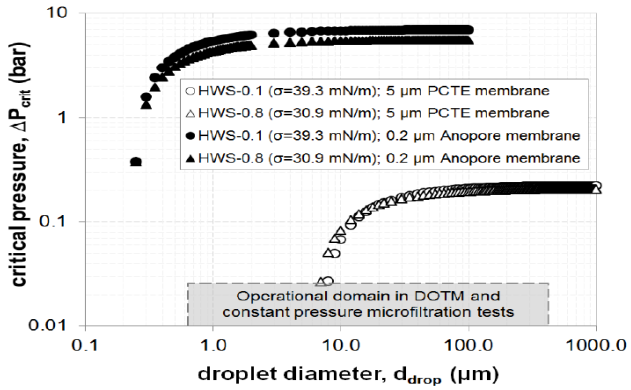

Fig 2.5 Critical pressure model evaluation. Adopted from Ref. [42]

Model interpretation and discussion

Darvishzadeh and Priezjec, conducted a computation Fluid dynamic (CFD) simulation study to validated the critical pressure in equation (7), fortunately, the simulation model in absence of crossflow predicted the matching values given by the critical pressure model in equation (7) [42]. However, the study also illustrated by the plot in figure 2.5 above, that under subcritical pressure conditions, the pressure increase is directly proportional to crossflow velocity up to a certain predetermined critical pressure value which results in oil droplet breakthrough [42]. Furthermore, the oil droplet deformation and permeation by critical pressure effect was reported to be a function of shear rate for the oil droplet radius ranging from (1.5 – 2.5 μm) at constant membrane pore radius of 0.5μm [42].

The last observation is that, in absence of crossflow the oil droplet has low curvature interface with the membrane surface resulting higher critical pressure for larger droplets [42].

2.1.4 Model (III)

During filtration process, modelling the critical pressure effect on oil droplet break-through takes into consideration: geometrical (membrane pores size) and fluid properties. This analytical approach used to model the critical pressure effect uses the force balance model principle, which is based on Navier-Stokes equations [42]. The schematic illustration of force balance model is shown below in figure 2.6[42]. The addition external factors which are also taken into consideration by this modelling approach are: flow velocity, drag force, surface tension and varying pressure on the membrane pore. This modelling approach to evaluate the critical pressure effect on oil droplet break-through membrane pores was implemented on CFD software (ANSYS FLUENT) and Volume of Fluid (VOF) simulation packages [45]. In modelling Volume of Fluid flow in force balance, similar modelling technique from model (I and II) were adopted. However, the only difference is the common transfer equation was coupled with volume fraction (α) to specify the oil/water interface taken into consideration, therefore for filtration phase the continuity equation was obtained as follows below[42, 46];

$$\frac{\partial\alpha}{\partial t}+\nabla\cdot\left(\alpha V\right)=0 \quad (1)$$

Whereby (V) is the velocity vector. The concentration polarization effect on the membrane surface was based on volume fraction and was assumed to average within each cell. The average feed density was obtained as follows:

$$\rho=\alpha\rho_w+\left(1-\alpha\right)\rho_{oil} \quad (2)$$

Combine equation (1) and (2) to obtain the momentum equation in equation (3) as follows

$$\frac{\partial}{\partial t}\left(\rho V\right)+\nabla\cdot\left(\rho V^2\right)=-\nabla P+\nabla\cdot\left[\mu\left(\nabla V+\nabla V^T\right)\right]+\rho g+F$$

Whereby (g) is gravitational acceleration, (F) is the surface tension force which is expressed in terms of oil/water interface as follows:

International Journal of Emerging Technology and Advanced Engineering
Website: www.ijetae.com (E-ISSN 2250-2459, Scopus Indexed, ISO 9001:2008 Certified Journal, Volume 12, Issue 07, July 2022)

$$F = \sigma \frac{\rho \nabla \alpha}{\frac{1}{2}(\rho_w + \rho_{oil})} \quad (4)$$

Considering the oil droplet at the entrance of the single pore on the schematic illustration in figure 2.6below: The drag force and capillary force were the main counteracting forces to determine the critical pressure required to cause the oil droplet breakthrough

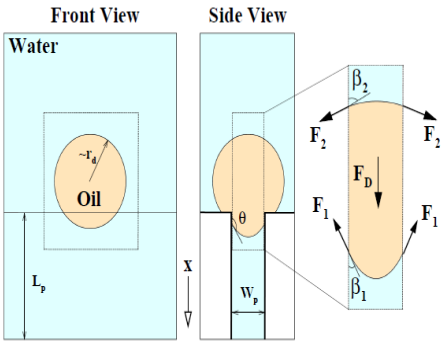

Fig 2.6 Schematic illustration of oil droplet permeation. Adopted from Ref.[42]

Despite the small Reynolds number due to laminar flow experience within the pore length, the drag force exerted by this viscous flow was assumed to be directly proportional to viscosity oil/water ratio, average flow velocity, oil droplet radius and water viscosity as follows.

$$F_D \propto f(\lambda)\mu_w \bar{u} r_d \quad (5)$$

Whereby (λ) is the oil/water ratio, (μ_w) is the water viscosity and $(\bar{u})$ is the average flow velocity. The flow velocity is proportional to the pressure gradient, as result, the high velocity (turbulent flow) induced on pore entrance is significantly reduce to a low velocity (laminar flow) inside the pore. This velocity parabolic profile inside pore is explained by Hagen-Poiseuille flow induced by planar pressure gradient. Consequently, the average velocity inside the pore is assumed to be proportional to the following

$$\bar{u} \propto \frac{W_p^{\,2}|\Delta P|}{\mu_w L_p} \quad (6)$$

Whereby (L_p) and (W_p) are pore length and width respectfully and (ΔP) is the static differential pressure of pore length. The critical pressure is determined from this static pressure. By substituting the average velocity from equation (6) in equation (5) the drag force is expressed in terms of static pressure as follows:

$$F_D \propto \frac{f(\lambda) W_p^{\,2} |\Delta P| r_d}{L_p} \quad (7)$$

From the schematic illustration in figure 2.3, considering only forces acting in (x) direction. The drag force is counteracted by vertical components of surface tension (F_{1x} and F_{2x}). Whereby $F_{1x} \approx 4 r_d \sigma \cos\beta_1$ and $F_{2x} \approx 4 r_d \sigma \cos\beta_2$, σ is surface tension coefficient, $\beta_1 = 180 - \theta$ and $\beta_2 \approx \cos^{-1}\left(\frac{W_p}{2r_p}\right)$ are extracted from contact angles. Therefore, the summation ofsurface tension force in vertical direction is given as follows:

$$F_{\sigma x} \approx 2\sigma W_p \left(\frac{2r_d \cos\beta_1}{W_p} - 1\right) \quad (8)$$

To satisfy critical pressure, the drag force in equation (7) should be equal or greater than the surface tension force in equation (8) $F_D = F_{\sigma x}$ after equating and rearranging the differential pressure inside the pore is made subject of the formula as follows

$$\Delta P = K \frac{\sigma\left(2r_d \cos\beta_1 / W_p - 1\right) L_p}{f(\lambda) W_p r_p} \quad (9)$$

Whereby (K) is the proportionality constant. To cater for pressure variation inside the pore,the pressure proportionality to pore size, $\left(\frac{r_d}{L_p}\Delta P\right)$ is added to the static pressure(ΔP) in equation (9). After rearranging equation (9) the critical pressure is made subject of the formula, the critical pressure model is obtained as follows [42].

$$P_{cr} = K \frac{\sigma\left(2r_d \cos\beta_1 / W_p - 1\right) L_p}{f(\lambda) W_p r_d \left(1 + r_d / L_p\right)} \quad (10)$$

International Journal of Emerging Technology and Advanced Engineering
Website: www.ijetae.com (E-ISSN 2250-2459, Scopus Indexed, ISO 9001:2008 Certified Journal, Volume 12, Issue 07, July 2022)

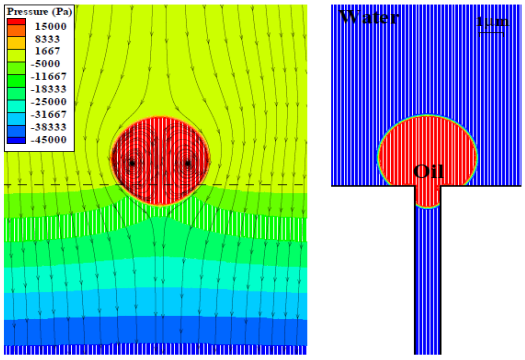

Fig 2.7 Numerical simulation results. Adopted from Ref. [42]

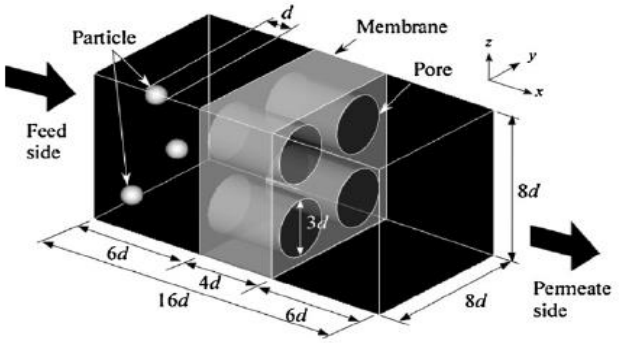

Fig 2.8 Computational domain of a membrane. Adopted from Ref. [1]

Discussion and interpretation of results

The theoretical prediction and numerical analysis based on Navier-Stokes laws, CFD simulation and Volume of Fluid method. It was discovered that the critical pressure was a function of surface tension coefficient, contact angle, oil/water viscosity ratio and oil droplet radius [42, 47]. However, recent numerical simulation as illustrated by figure 2.7 above, have proven that the critical transmembrane pressure in cross flow application is significantly higher than dead-end configuration due to increased drag force generated by the shear flow. In addition, numerical simulation investigated the effect of each parameter in equation (10). Itwas indeed discovered that the oil droplet permeation by critical pressure is predominantly influenced by the contact angle, oil droplet/pore ratio and surface tension.

2.1.5 Model (IV)

[1]conducted a modelling and simulation study to investigate fouling resistance accumulation and removal. The investigation were based on pressure-driven, dead-end microfiltration and backwash cleaning efficiency respectively. Furthermore, to evaluate the fouling effect on membrane pore size, this study was addressed on two fronts. Firstly, the pore size was assumed to be more than twice the size of a foulant, secondly the pore size was assumed to be less than four-times the size of a foulant particle. Consequently, cake layer build-up on the membrane surface was considered to be the only dominant fouling formation compared with other conventional fouling formation models (complete and standard blockage)[1]. Membrane developed model, was a four regular spaced cylindrical track-etched pores as illustrated by the schematic diagram in figure 2.8 below[1].

2.1.5.1 Model development

Both solvents and foulant particles flow were developed based on the momentum equation governed by Navier-Stokes equation as follows[1].

$$\frac{\partial v}{\partial t}+(v\cdot\nabla)v=-\frac{1}{\rho}\nabla P+\frac{\mu}{\rho}\nabla^2 v+\frac{1}{\rho}\nabla\cdot S-\frac{1}{\rho}D+\Phi\alpha \qquad (1)$$

$$\alpha=\frac{v^F-v^{NF}}{\Delta t}+(v\cdot\nabla)v-\frac{\mu}{\rho}\nabla^2 v-\frac{1}{\rho}\nabla\cdot S+\frac{1}{\rho}D \qquad (2)$$

Whereby: (v) is the fluid velocity, (ρ) is the solvent density, (P) is the static pressure, (μ) is the solvent viscosity, (D) is the pressure gradient vector, (S) is the fluctuating thermal stress tensor, (Φ) is the volume ratio of foulants and membrane coverage and (α) is the acceleration vector of foulants. To satisfy the mass conservation laws, static pressure is subdivided into two: which is the intermediate pressure without foulants $\left(P^{NF}\right)$ and correcting pressure with foulants $\left(P^{F}\right)$.

$$P=P^{NF}+P^{F} \qquad (3)$$

By substituting equation (2) and (3) into (1), the following flow velocity without particles was obtained in equation (4) below[1]:

$$\frac{\partial v^{NF}}{\partial t}=(1-\Phi)\left[-(v^{NF}\cdot\nabla)v^{NF}+\frac{\mu}{\rho}\nabla^2 v^{\circ}+\frac{1}{\rho}\nabla\cdot S-\frac{1}{\rho}D\right]-\frac{1}{\rho}\nabla P^{NF}+\Phi\left(\frac{v^F-v^{NF}}{\Delta t}\right)-\frac{1}{\rho}\nabla P^{F}$$

Backwash flow media is regarded as pure solvent transport, therefore the continuity equation is expressed by

$$\nabla\cdot v^{NF}=0 \qquad (5)$$

International Journal of Emerging Technology and Advanced Engineering
Website: www.ijetae.com (E-ISSN 2250-2459, Scopus Indexed, ISO 9001:2008 Certified Journal, Volume 12, Issue 07, July 2022)

During filtration phase, the flow media with foulants is expressed by

$$\nabla \cdot v^{n+1} = 0 \qquad (6)$$

Introducing the gradient operator on both sides of the equation (4) and taking into consideration equation (5), for pure solvent transport during backwash, the Poisson equation of backwash-pressure is obtained as follows in equation (7)[1]:

$$\nabla^2 P^{NF} = \rho\left[\frac{\nabla \cdot v^n}{\Delta t} + \nabla \cdot \left\{(1-\Phi)\left(-\left(v^{NF}\cdot\nabla\right)v^{NF} + \frac{\mu}{\rho}\nabla \cdot v^{NF} + \frac{1}{\rho}\nabla \cdot S - \frac{1}{\rho}D\right)\right\}\right]$$

Taking into consideration equation (6), the flow media with foulants and introducing the gradient operator on sides of equation (4), the following expression is obtained[1].

$$\nabla^2 P^F = \rho\left[\frac{\nabla \cdot v^{NF}}{\Delta t} + \nabla \cdot \left(\Phi \frac{v^F - v^{NF}}{\Delta t}\right)\right] \qquad (8)$$

2.1.5.2 Motion of foulants

The translation motion of (l-th) foulant particles in a solvent is governed by Newton's law of motion, which is expressed by the following equation[1].

$$m_i \frac{dV_i}{dt} = F_i^c + F_i^e + F_i^h + F_i^{lb} \qquad (9)$$

Whereby: $\left(m_i\right)$ represents the mass of foulant, (V_i) is the foulants translational velocity vector, $\left(F_i^c\right)$ is the contact force, $\left(F_i^e\right)$ is the electrostatic force, $\left(F_i^v\right)$ is the van derWaals force, $\left(F_i^h\right)$ represents the hydrodynamic force and $\left(F_i^{lb}\right)$ represents the lubricative forces[1].

The rotational motion of foulants is expressed as follows

$$I_i \frac{d\omega_i}{dt} = T_i^c + T_i^h \qquad (10)$$

Whereby (I_i) represent the moment of inertia of foulants, $\left(\omega_i\right)$ is the foulant angular velocity, $\left(T_i^c\right)$ and $\left(T_i^h\right)$ represent the contact and hydrodynamic torque.

The contact force and torque are derived from Voigt model, Hertzian theory and Mindlin model[1]. The interface force combining the electrostatic and van der Waals forces between foulants and membrane structure is given by Derjaguin Landau Verwey Overbeek (DLVO) theory[1]. In addition, the lubricating interface force between foulant has been considered to be a dominant force for scales that are smaller than the lattice resolution[1]. The volume integration of $\left(\alpha\right)$ was used to derive the hydrodynamic force and torque as follows[1]:

$$F_i^h = -\int_{v^F} \Phi_i^F\left(r\right)\left[\rho\alpha\left(r\right) + D\right]dV \qquad (11)$$

$$T_i^h = -\int_{v^F} \Phi_i^F\left(r\right)\left[r_i\left(r\right) \times \rho\alpha\left(r\right)\right]dV \qquad (12)$$

Whereby $\left(V^F\right)$ represented the membrane volume region occupied by the foulants. The hydrodynamic force, torque and stochastic fluctuating stress demonstrate the diffusion effects of particles[1].

2.1.5.3 Numerical analysis

First order Euler explicit equations was used to solve the rotational and translational motion of faulants and the position of foulants was solved by Crank-Nicolson equations[1]. Navier-stokes equations were solved by two-step procedure: first, the Semi-implicit method for pressure-linked equations (SIMPLEST), followed by convergence algorithm method using the iterative calculation of pressure.In this study, the objective was evaluate the effect of fouling phenomenon on membrane pore size by comparing obtained simulation results (snapshots) of foulants accumulation and removal over a certain period[1].

2.1.5.3 Simulation results

The measurable pore size and porosities of each pore were as follows: $2.5d(250nm)$, $\varepsilon = 0.306$ and the standard pore size $3d\left(360nm\right), \varepsilon = 0.441$ and $\varepsilon = 0.636$ respectively. The permeate flux is given by the average flow rate passing through the pore divided by the effective cross-sectional area of membrane.

International Journal of Emerging Technology and Advanced Engineering
Website: www.ijetae.com (E-ISSN 2250-2459, Scopus Indexed, ISO 9001:2008 Certified Journal, Volume 12, Issue 07, July 2022)

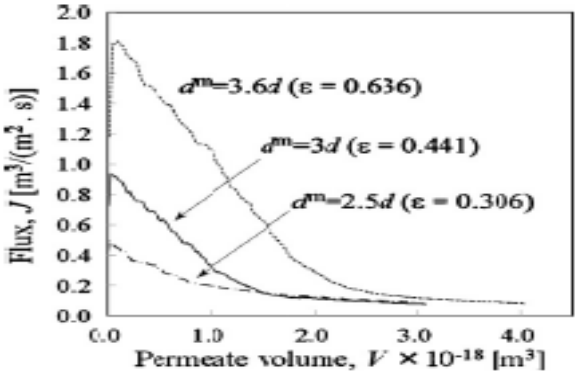

Fig 2.9 Permeate flux as function of permeate volume. Adopted from Ref. [1]

The permeate flux data was used to evaluate the fouling condition by plotting permeate flux as function of permeate volume as shown in figure 2.9 above. Each pore draws an independent permeate flux curve demonstrating that, when the permeate volume increases the respective pore flux is decreased proportionally. To incorporate backwash effect on permeate flux recovery as shown in figure 2.8.

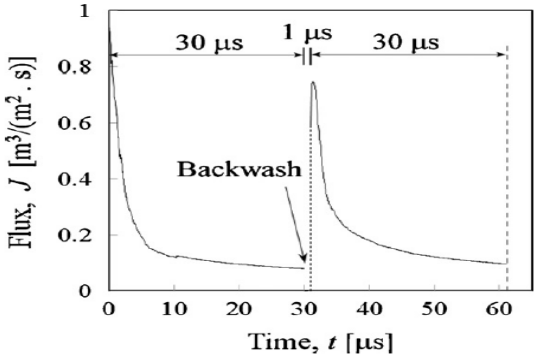

Fig 2.10 Permeate flux fluctuation. Adopted from Ref. [1]

Backwash simulation was performed after $(30\mu s)$ ofa normal filtration operation, under which a fixed foulant concentration $(\phi = 5\%)$. Back-pressure was reported to be eight times that of filtration operation and the backwash duration was $(1\mu s)$ as shown in figure 2.10 which also demonstrated the permeate flux decline and recovery through a sequence of filtration and backwash respectively[1].

By comparing the fouling formation before and after backwash operation, the following conclusion were drawn: reversible foulants found on the membrane structure after performing inadequate backwash procedure may gradually evolve into irreversible foulants.

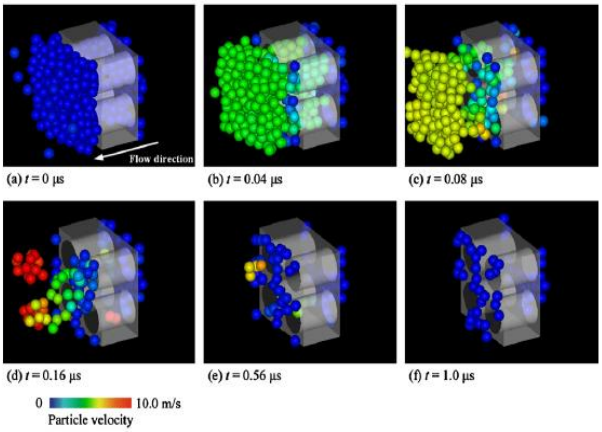

Fig. 2.11 Snapshots illustrating backwash simulation. Adopted from Ref.[1].

2.1.5.4 Discussion and interpretation of simulation results

Figure 2.11 above illustrates the snapshots of a backwash simulation through a velocity profile which demonstrates foulants removal on the membrane structure with respect to time[1]. Initially there is no foulant motion, but after $(0.04\mu s)$ both foulants on the pore and surface of the membrane have a finite velocity. The foulants on feed-side form a large cluster before been removed as shown below. Due to inadequate backwash procedure, some foulants remain on the membrane permeate side-surface and inside the pores as shown by (figure 2.11) [1]. As a result, foulant starts the adhesion and clogging (polarization concentration) of the membrane surface and pores by these small foulants which accumulates and evolves into irreversible foulants. The irreversible foulant due to their stubborn nature to resist cleaning, reduces membrane permeability and separation efficiency. Consequently, affecting the membrane performance by reducing the productivity, permeate quality and the effective membrane pore area forcing a change in fouling formation from pore blockage and cake layer build-up to cake layer formation only[1].

International Journal of Emerging Technology and Advanced Engineering
Website: www.ijetae.com (E-ISSN 2250-2459, Scopus Indexed, ISO 9001:2008 Certified Journal, Volume 12, Issue 07, July 2022)

2.1.5.5 Conclusion

Membrane fouling was examined by evaluating the following operating conditions: fouling motion, permeate flux fluctuations and membrane resistance accumulation over a certain filtration period.Based on the obtained results, the foulant motion confirmed two modes of fouling formation. Firstly, the foulants begin by filling the pores (pore blockage) followed by the cake layer accumulation on membrane surface. Secondly, cake layer build-up on the membrane surface considered to be the only the dominating fouling formation without pore blockage. The first mode of fouling formation was experienced on a larger pore size while the second mode of fouling formation was experienced on a smaller pore size of varying pore size microfiltration.

2.2 Sub-section two

In the past numerous efforts have been made towards developing an improved backwash cleaning efficiency. This sub-section outlines the procedures, methods, materials and protocol carried out during some of the experimentation studiesto evaluate some of the identified operating parameters in backwash optimization.

2.2.1 Experiment study (I)

Hua *et al.*(2007) Conducted an experiment study on oily wastewater by cross-flow microfiltration (MF) using a ceramic (alfa-Al_2O_3) membrane of 50mm pore size[48, 49]. In this study, the influence of operating parameters such as temperature, trans-membrane pressure, cross-flow velocity and feed oil concentration were evaluated. The dynamic relationship of the above mentioned parameters was investigated by measurements of the: Total organic carbon (TOC) separation efficiency and permeate flux. The following tables of results were obtained [49].

2.2.1.1 The effect of Trans-membrane Pressure (TMP)

The adaptive constant experiment condition were as follows CFV=1.68 ms^{-1}, oil concentration 500 mgL^{-1}. The following table of results was obtained under vary Transmembrane pressure (TMP)[48, 49].

TABLE 2.2.1
TMP EFFECT

No table of figures entries found.	0.05	0.1	0.15	0.2
Flux ($Lm^{-2}h^{-1}$)	30	70	110	170
TOC separation efficiency (%)	97.3	97	95.2	93

Discussion and interpretation of results

The results conclude that, high permeate flux is achievable under high transmembrane pressure, high CFV and low oil concentration. Results also indicate that TOC separation efficiency were above 90% in all experiments, which were an expected values. However, it was also discovered that an increase in (TMP) resulted in decrease of the TOC separation efficiency due to the probability increase of oil droplet breakthrough.

2.2.1.2 The effect of Cross-flow Velocity (CFV)

The adaptive constant experiment condition by Hua *et al.* (2007) were as follows TMP=0.2bar oil concentration 500 mgL^{-1}.The varying CFV was applied ranging from 0.17 to 1.7 ms^{-1} as shown in table 2.2.2 below [48]

TABLE 2.2.2
CFV EFFECT

Cross flow velocity (ms^{-1})	0.17	0.42	0.8	1.7
Flux ($Lm^{-2}h^{-1}$)	122	135	140	165
TOC separation efficiency (%)	97.5	97.4	97.5	97.4

Discussion and interpretation of results

The results demonstrated that increase in CFV led to steady increase in permeate flux as explained by Reynolds number laws. The results also indicate steady TOC separation efficiency above (97%) overall.

2.2.2 Experiment study (II)

Tompkins *et al.*(2007)Also conducted a short experimentation study to determine the relationship between the permeate flux rate and the associated fouling. The experiment set-up consisted of dense-pack ceramic ultrafiltration membrane of about 11.2 m^2 surface area [49, 50]. The experiment test was conducted in similar manner to that of Hua *et al* except the permeate flow rate was kept constant by throttled valves of the system

Effects of membrane fouling on permeate flux [50].

TABLE 2.2.3
PERMEATE FLUX

Flux $Lm^{-2}h^{-1}$	Allowable membrane resistance $(barL^{-1}m^{-2}h^{-1})$	Estimated lifespan (hrs)
51	0.08	3.55
76	0.05	2.5
102	0.04	3.8
127	0.03	1.35
153	0.02	2.00

International Journal of Emerging Technology and Advanced Engineering
Website: www.ijetae.com (E-ISSN 2250-2459, Scopus Indexed, ISO 9001:2008 Certified Journal, Volume 12, Issue 07, July 2022)

Discussion and interpretation of results

The results indicate that the maximum estimated life-span can be achieved at the permeate flux rate of 102 $Lm^{-2}h^{-1}$ which is associated with the highest estimated lifespan, in comparison with the tabled results.

2.2.3 Experiment study (III)

The objective of the experimentation study was to investigate the effects of operating parameters such as temperature, pressure, fouling resistance and flow velocity on TOC separation efficiency[51]. As such the parameters were adjusted using the system regulators, in search of the critical operating condition. The initial test were conducted with pure water to attain the pure permeate flux to be used as reference. A tubular alpha ceramic membrane with pore size $0.2\mu m$ model (MF190) supplied by $FILTEC^{TM}$ Ceramic Membrane Company was used [51]. The oil/water feed was artificial processed mixture. From the initial test conduct using pure water, membrane resistance (R_m) was calculated using the model equation below [51].

$$R_m = \left(\frac{\Delta P}{\mu J_{wi}}\right)\left(\frac{1}{m}\right) \qquad (1)$$

From equation (1), The accumulated resistance (R_f) during filtration phase can be calculated using the following equation [51]

$$R_f = \left(\frac{\Delta P}{\mu J_{ww}}\right) - R_m\left(\frac{1}{m}\right) \qquad (2)$$

Grease &oil content and Total Organic Carbon (TOC) tests and analysis were performed on the feed and permeate sample. The separation efficiency was then evaluated by TOC separation efficiency R_{TOC} value as follows [51]

$$R_{TOC} = \left(\frac{TOC_{feed} - TOC_{permeate}}{TOC_{feed}}\right)\times 100 \qquad (3)$$

Whereby TOC_{feed} and $TOC_{permeate}$ represent the feed and permeate TOC concentration (mg/L) respectfully.

2.3.3.1 Effects of transmembrane pressure

To investigate the effect transmembrane pressure on: TOC separation efficiency, permeate flux, and fouling resistance.

Series of experiment were conducted, in which TMP was varied from (0.75-1.75bar), under which the operation conditions such as Temperature $(32.5^{\circ}c)$ and CFV $(2.25m/s)$ were kept constant. The graphical representation below was obtained [51].

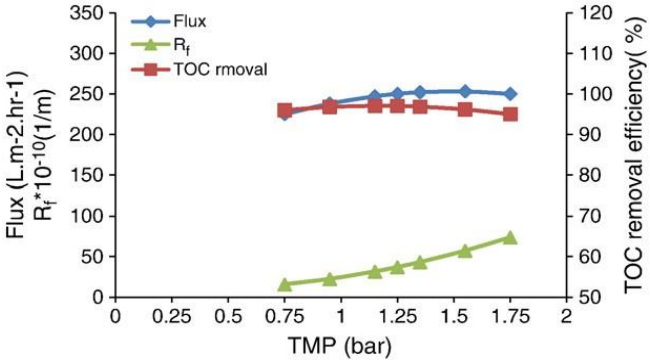

Fig 2.2.4 EffectsofTMPonpermeateflux,TOCandR$_f$. Adopted from Ref.[51]

Discussion and interpretation of results

Based on Darcy's laws (at low TMP the permeate flux is directly proportional to TMP), results indicate that an increase in TMP results in increase of permeate flux [52]. However excessive TMP increase results in compressed concentrated polarization of foulant on the membrane, which as result increases the probability of foulant/oil droplet breakthrough on the membrane [53]. On the contrary, the oil droplet breakthrough reduce the TOC separation efficiency, as indicate by the reduction in efficiency for TMP higher than (1.25 bar). The results also indicate an increase in TMP results in increase in fouling resistance, this is due to increase in of accumulation of foulant layer (formation of cake/gel layer) on membrane surface. TMP of **1.25 bar** was recommended to be an optimal pressure for effective operating conditions [51].

2.3.3.2 Effect of Cross flow velocity

The objective was to investigate the effect of CFV on: permeate flux, fouling resistance and TOC separation efficiency. Similar to set of experiments on conducted on investigating the effect of TMP. However, the only difference is CFV was the varied parameters from (0.75-2.25m/s), while TMP of (1.25bar) and temperature $(32.5^{\circ}c)$ were throttled to a constant operation.

International Journal of Emerging Technology and Advanced Engineering
Website: www.ijetae.com (E-ISSN 2250-2459, Scopus Indexed, ISO 9001:2008 Certified Journal, Volume 12, Issue 07, July 2022)

The following graphical representation of results was obtained [51].

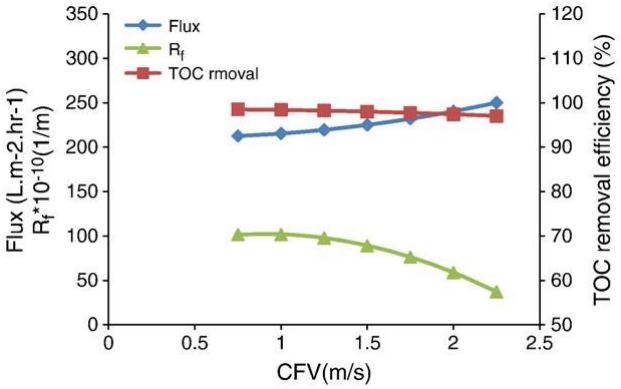

Fig.2.2.5 EffectsofCFVonpermeateflux,TOCandR_f. Adopted from Ref.[51]

Discussion and interpretation of results

The results indicate that an increase in CFV results in increase of permeate flux, due to increase of turbulence and mass transfer coefficient based on Darcy's laws [54]. The result also indicate decrease in fouling resistance as the accumulation of foulants on the membrane surface are easily swept back into feed tank by high CFV (2.25 m/s). On the contrary, increase in CFV resulted in a slight decrease of TOC separation efficiency due high shear rate that eliminates the accumulation of foulant (that actas a sub-filter layer) on membrane surface. As consequence, organic matter can easily pass through the membrane and reduce the separation efficiency [52, 55]. In conclusion, the CFV of 2.25m/s was recommended to be an optimal operating condition, due high permeate flux and low fouling resistance it poses as indicate by the results[51].

2.3.3.3 Effect of temperature

The effect of temperature on: TOC separation efficiency, fouling resistance and permeate flux was investigated. In this series of experiments, under which temperature was varied from (25-40˚c) while other operating parameters such as TMP (1.25 bar) and CFV (2.25m/s) were kept constant during this set of experiments, the set of results were plotted as follows [51]:

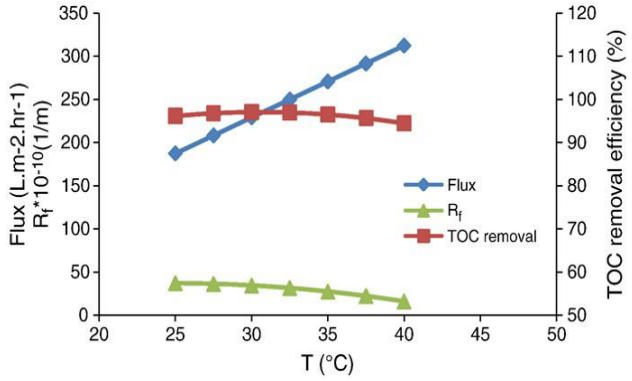

Fig 2.2.6.EffectsofTemp.on thepermeatefluxand TOC. Adopted from Ref.[51]

Discussion and interpretation of results

The results show an increase temperature results in increase of permeate flux, due decrease in oil viscosity [56]. However, this viscosity reduction effect results in decrease of fouling resistance and TOC separation efficiency [57]. Based on the results temperature of $32.5^{\circ}c$ was recommended to be an optimal operating condition [51].

2.3.3.4 Effect of backwash on permeate flux recovery

The set of experiments were carried to investigate the effect of backwash on permeate flux recovery. In this series of experiments, parameters such as TMP (1.25 bar), CFV (2.25 m/s) and temperature ($32.5^{\circ}c$) were utilized as optimal operating parameters. The first 40 min results of the long-term operation was plotted below [51].

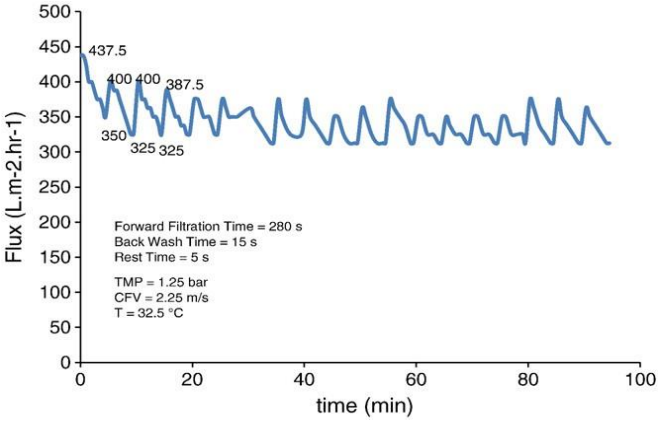

Fig 2.2.7 Effectofbackwashing on fluxdecline. Adopted from Ref.[51].

International Journal of Emerging Technology and Advanced Engineering
Website: www.ijetae.com (E-ISSN 2250-2459, Scopus Indexed, ISO 9001:2008 Certified Journal, Volume 12, Issue 07, July 2022)

Discussion and interpretation of results

The results indicate a significate permeate flux recovery (over 95% of the original flux) by periodic backwash process. The dynamic relationship of the recommended critical operating parameters such as temperature ($32.5^{\circ}c$), TMP (1.25 bar) and CFV (2.25 m/s) of backwash media has proven to be sufficient to maintain optimal results for a long-term operation [51].

Section B

III. Permeate Flux Models

The complexity of filtration and backwash can reduce by modelling [6]. As demonstrated, the efficiency of backwash depends on varies parameters. Modelling helps identify the effect of these parameters (individual and collectively) on varying operation conditions. The reliable model not only can they safe time, but can also reduce cost associated with multiple experiments required to obtain optimal operating condition for improved backwash process [6].

3.1 Application of permeate flux models

The most interesting aspect in integrating filtration, backwash and fouling models is flux prediction models [6]. The net permeate flux is the total permeate collected during the filtration phase minus the utilised total fluid used during backwash phase over the entire experiment period [6]. The initial reasonable prediction accuracy of the net permeate flux models was based on lab-scale constant-pressure mode during both filtration and backwash [58]. Redkar et al. (1996) derived the net permeate flux model under the assumption that backwash cleaning process restores the net permeate flux (J) to its initial value, in other words maintenance flux recovery of 100% for each and every cleaning procedure [58].

$$J = \frac{\int_0^{t_f} J_f(t)dt - \int_{t_f}^{t_f+t_b} J_b(t)\,dt}{t_f + t_b} \qquad (1)$$

Whereby the (J_f) and (J_b) are filtration and backwash permeate flux respectively and also (t_f) and (t_b) are time duration for filtration and backwash phase respectively.

In equation (1), the net permeate flux (J) is a dependent variable while filtration duration (t_f) is an independent variable which is related to the backwash duration by the following equation: $t_f = 1/f - t_b$ and (f) represents the backwash frequency.

3.2 Analytical model approach

In attempt to simplify the net permeate flux model in equation (1) six analytical modification models were developed based on Darcy's laws and Blake-Kozeny equation (on cake layer resistance) [6, 59, 60].

3.2.1 Model (I)

The first assumption when deriving the model was that the membrane fouling is instantly removed by backwash thus produce a 100% flux recovery equivalent to the initial flux (J_0) by pure water [6]. The second assumption is that the filtration permeate flux decline was only caused by cake layer formation type of fouling on a dead-end filtration configuration [59].

$$J_f = J_0 / \left(1 + t_f / \tau_1\right)^{1/2} \qquad (2)$$

Whereby (τ_1) is the permeate flux decline time constant. To take into account the CFV configuration. [61]derived a semi-empirical equation for filtration permeate flux decline as follows.

$$J_f(t) = \frac{J_0 - J_s}{\left(1 + t_f / \tau_1\right)^n} + J_s \qquad (3)$$

Whereby (n) and (τ_1) are regression constants, (J_s) is the steady-state permeate flux. The permeate flux decline constant (τ_1) was derived by Murkes and Carlson with the assumption of cake layer formation of standard fouling theory [62]:

$$\tau_1 = \frac{(C_C - C_B)\Delta P_f}{2\gamma\mu C_B J_0^{\,2}} \qquad (4)$$

Whereby (C_B) and (C_C) are cake bulk solute concentration and solute concentration respectively, (ΔP_f) is filtration TMP, (γ) is the specific cake layer resistance per unit depth and (μ) is the feed viscosity.

International Journal of Emerging Technology and Advanced Engineering
Website: www.ijetae.com (E-ISSN 2250-2459, Scopus Indexed, ISO 9001:2008 Certified Journal, Volume 12, Issue 07, July 2022)

For backwash flux, it is assumed the only resistance experienced by the reverse flow is the membrane resistance. Therefore backwash flux is equal to initial flux of a clean membrane

$$J_b = \frac{\Delta P_b}{\mu R_m} = \frac{\Delta P_b}{\Delta P_f} J_0 = \alpha J_0 \qquad (5)$$

Whereby (ΔP_b) is the applied reverse pressure and (α) is the ratio between filtration TMP to reverse pressure.

After substituting and manipulating equation (2) and (5) in equation (1) the following corresponding net permeate flux was obtained

$$J = J_0 \frac{2\tau_1\left[\left(1+t_f/\tau_1\right)^{1/2}-1\right]-\alpha t_b}{t_f+t_b} \qquad (6)$$

3.*2.2 Model (II)*

Model (I) was further modified to take into account the fouling removal during backwash does not happen instantly, as such backwash duration was taken into consideration. Therefore alteration were introduced on the reverse flux as follows:

$$J_b(t) = \alpha J_0\left[1-\left(1+t_b/\tau_2\right)^{-1/2}\right] \qquad (7)$$

Whereby (τ_2) is the reverse flux time constant increase during cake foulant removal. Substituting equation (7) in the net permeate flux is obtained as follows in equation (8).

$$J = J_0 \frac{2\tau_1\left[\left(1+t_f/\tau_2\right)^{1/2}-1\right]-\alpha t_b+2\alpha\tau_2\left[\left(1+\left(t_f+t_b\right)/\tau_2\right)^{1/2}-\left(1+t_f/\tau_2\right)^{1/2}\right]}{t_f+t_b}$$

3.2.3 Model (III)

To take into consideration the inefficient cleaning procedure Kuberkar et al. (1998) develpop a model to incorporate the irreversible fouling as result of incomplete or insufficient backwash [26]. The cleaning efficiency parameter (β) was introduced, which is defined as the ratio of cleaned surface area to total surface are of the membrane. The assumption was the cleaned portion has 100% permeate flux recovery equivalent to initial flux (J_0), while the uncleaned portion maintains a long-term resistance or steady state resistance (J_s). The filtration and backwash flux were composed through the cleaning efficiency as follows [26]:

$$J_f(t) = \beta J_0/(1+t_f/\tau_1)^{1/2} + (1-\beta)J_s \qquad (9)$$

$$J_b(t) = \alpha\beta J_0 + \alpha(1-\beta)J_s \qquad (10)$$

After substituting and manipulating equation (9) and (10) in equation (1) the corresponding net permeate flux was obtained in equation (11) below.

$$J = \beta J_0 \frac{2\tau_1\left[\left(1+t_f/\tau_1\right)^{1/2}-1\right]-\alpha t_b}{t_f+t_b} + (1-\beta)J_s\frac{\left(t_f-\alpha t_b\right)}{t_f+t_b}$$

3.2 Discussion and interpretation of models

The feasible application of these models is to predict flux decline and recovery in various filtration and backwash processesrespectively. The four models were implemented on multiple experiments that was summarized in a review study by Gao et al.(2019)[6]. These models were evaluated on lab-scale under constant pressure operating conditions. To identify the most accurate model, net permeate flux prediction accuracy for each models were evaluated and compared by mean absolute deviation (MAD) concept and simulated using MATLAB. The simulationresults above indicate model (II and III) were a great improvement for Model (I) by taking into account the cleaning efficiency (β). However, models (II) is marginally worse in comparison to model (III) on net flux prediction. Due to similar assumption between models, they therefore adopt similar filtration and backpulse flux except in model (III) the modified cleaning efficiency (β_b) is introduced instead of just (β) On the contrary, the prediction accuracy of the models vary depending on the type application. Even though this model were developed to be implemented on the backpulse system. However, the fundamental principle of operation between backwash and backpulse permits adaptation of this model to a backwash system, as they were developed based on Blake-Kozeny (fouling formation) and Darcy' law.

3.2 Experimental model approach

In the past, numerous efforts have been made towards developing theoretical modelling for both fouling and backwash phenomenon. Further investigation on this models lead to new discoveries, such as: predictable of flux recovery and decline models based on experimental findings [19]. To determine the cleaning efficiency of backwash system on any cleaning method in membrane technology, the flux recovery model and the fouling models were developed by several experimentation studies.

3.3.1 Model (I)

International Journal of Emerging Technology and Advanced Engineering
Website: www.ijetae.com (E-ISSN 2250-2459, Scopus Indexed, ISO 9001:2008 Certified Journal, Volume 12, Issue 07, July 2022)

The fundamental application of flux recovery and fouling models is to evaluate the cleaning efficiency. developed flux recovery and decline based on the following ratio [63]:

$$\text{Flux recovery} = J_c / J_0 \qquad (1)$$

$$\text{Fouling ratio} = J_f / J_0 \qquad (2)$$

Whereby (J_f), (J_c) and (J_0) are flux of fouled membrane, membrane flux after cleaning and initial flux of membrane respectively.

3.3.2 Model (II)

The second expression defined as Pure water flux reduction (FRED) was developed to evaluate cleaning efficiency by [64].

$$\text{FRED}(\%) = 100\left(J_0 - J_f\right) / J_0 \qquad (3)$$

[65] developed an express to evaluate backwash efficiency as:

$$n = \frac{100\left(P_f - P_c\right)}{\left(P_f - P_0\right)} \qquad (4)$$

Where (P_f), (P_c) and (P_0) are pressure applied on the fouled, cleaned and initial membrane respectively.

3.3.4 Model (III)

[66] developed two expressions to investigate chemical cleaning efficiency of RO membrane, which are resistance removal $(RR\%)$ and flux recovery $(FR\%)$

$$RR\% = 100\left[\left(R_f - R_{ir}\right) / R_f\right] \qquad (5)$$

$$FR\% = 100\frac{\left(J_c - J_{wf}\right)}{\left(J_0 - J_{wf}\right)} \qquad (6)$$

Where (R_f), (R_{ir}) and (J_f) are fouled resistance, irreversible fouling and fouled membrane permeate flux.In addition, Wu and [67] developed a Fouling resistance recovery model (FRR) to investigate the cleaning efficiency based on the ultrafiltration system.

$$FRR\% = 100\left[\left(R_f - R_c\right) / \left(R_f - R_0\right)\right] \qquad (7)$$

Where (R_f) and (R_c) are pure water flux resistance of a fouled and cleaned membrane.

3.4 Discussion and interpretation

There are two kinds of applications of these experimental models. First is evaluate the effect of cleaning efficiency on flux recovery by backwash and chemical agents. Secondly, is to understand the processes involved in fouling formation on the membrane. The model application incorporates membrane filtrations with backwash systems to evaluate both flux decline and recovery during experimentation

3.5 Conclusion

The evaluation of critical parameters by models offers insight into the backwash and fouling action mechanisms. For backwash can be optimized by adjusting the following parameter, pressure, temperature, duration, frequency and backwash media, till the required operating condition that are capable to achieve maximum flux recovery. Recent studies have demonstrate that up to around 95% of permeate flux recovery is achievable by deploying backwash [51]. The continuous permeate flux recovery of 95% reduces the probability of irreversible fouling accumulation very significantly[4]. The integrative approach of identifying this models is focused on the attempt to cover all relevant aspects of the backwash techniques being considered in optimizing the backwash procedure. To evaluate the efficiency of backwash, in modelling and experimentation study, the applicability of these models is depict on the validation phase, where the performance of the developed backwash technique is evaluated in terms of permeation production. The other take from this model is that, experimental studies alone cannot completely evaluate the effectiveness of the backwash parameters, as these models have proven to be an effective approach to prediction, analyse and understand of dynamic relationship of the involved parameters during operation

Section C

IV. Fouling Models

Membrane fouling drawbacks: reduces water permeability and separation efficiency. As consequent, affect the membrane performance by reducing the life-span, productivity, and permeate quality, also increasing operation cost as well as a reduction in membrane lifetime [2].

Generally, membrane fouling arising from adsorption/deformation of oil droplets on the membrane surface[28]. Basically, during the process of oil/water

International Journal of Emerging Technology and Advanced Engineering
Website: www.ijetae.com (E-ISSN 2250-2459, Scopus Indexed, ISO 9001:2008 Certified Journal, Volume 12, Issue 07, July 2022)

separation by membrane filtration, the adhesion and clogging of the membrane surface pores by small oil droplets may result in fouling of membrane system (loss of water permeability and separation effectiveness) [68]. Removal of these oil droplets contaminates on the membrane surface is one of the most critical issues that needs to be addressed[2]. Generally, depending on the driving pressure and the tension forces on the membrane surface, oil droplets can be forced to deform and permeate through the pores[4]. In line with the aim to improve permeability and separation efficiency, this oil drop deformation effect will be considered in this investigation study, under which different methods and models will be developed to demonstrate its build-up.

The investigation of fouling models in this section is done for three purposes. Firstly, is to understand permeate flux decline during oil/water separation. Secondly is to have a thorough understanding of fouling phenomenon from fundamental principle to different types of fouling formation, based on the interaction with different operating conditions[4]. Thirdly, is to identify relevant fouling model that can be used to develop an optimized fouling removal or prevention technique[4]. To date, several modelling techniques have been used to model fouling, such as: block laws[69, 70], resistance [71, 72] neutral network[73, 74] and black box technique[75]. However, in this review only two of these techniques are discussed, namely: block laws and resistance-based modelling techniques. Generally, membrane blockage is classified by four fouling formation, namely: complete blockage, intermediate blockage, standard blockage and cake blockage as illustrated by the schematic diagram below [4].

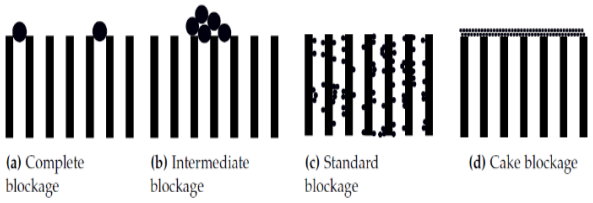

Figure 3.1 Block Models. Adopted from Ref. [4]

4.1 Blockage laws

Hermiaderived the simplified blockage models as follows [22].

$$\frac{d^2t}{dV^2} = \alpha\left(\frac{dt}{dV}\right)^n \qquad (1)$$

Whereby (n) defines the type of fouling formation as follows: $(n=0)$ is cake formation, $(n=1)$ is intermediate blockage, $(n=2)$ is complete blockage and $(n=3/2)$ is standard blockage. $\left(\frac{dt}{dV}\right)$ is the fouling resistance expression not a volume derivative of time. The model can further be simplified by expressing it in terms of resistance not time as shown by equation (1). Fouling resistance is generally define by equation (2) as follows[22].

$$\frac{dt}{dV} = \frac{1}{j} = \frac{R_t}{\Delta P} \qquad (2)$$

The second order derivative of fouling resistance model is formulate as follows:

$$\frac{d^2t}{dV^2} = \frac{d}{dV}\left(\frac{R_t}{\Delta P}\right) = \alpha\left(\frac{R_t}{\Delta P}\right)^n \qquad (3)$$

To express fouling resistance in terms of time (resistance accumulation over time), the constant TMP by blockage laws is assumed and the equation is multiple with $\left(\frac{dV}{dt}\right)$ on both sides of the equation to obtain equation (3) as follows[4]:

$$\frac{dR_t}{dt} = \alpha R_t^n j \qquad (4)$$

N.B equation (4) can be expressedexclusively by resistance (R_t) or membrane flux (j). For blockage models in this review, membrane flux was the exclusive parameter.

Hermia blockage laws were initially intended for modelling solid foulant on a dead-end filtration system[76, 77]. However, after realize the prediction accuracy of this block models, some modification were introduced to account for CF filtration and oil/water separation application[78, 79]. The initial assumption which now considered to be a main drawback on Hermia laws, is assuming operation parameters such as: feed concentration, TMP and temperature remain constant during filtration process (Jepsen et al., 2018).

One approach that help Hermia laws to be popularly applicable, was to estimate fouling coefficient for each specific operating parameter(Jepsen et al., 2018). However, the estimated fouling coefficients were found to be accurate only on a single CFV and a significant accuracy reduction

International Journal of Emerging Technology and Advanced Engineering
Website: www.ijetae.com (E-ISSN 2250-2459, Scopus Indexed, ISO 9001:2008 Certified Journal, Volume 12, Issue 07, July 2022)

was experience by the deviation from the define operating condition[80].

To date, Hermia blockage laws have been used in modelling fouling behaviour of oil/water separation[81, 82]. By identifying fouling coefficients, acceptable model accuracy has been achieved for each operating parameter and the developed prediction models using those fouling coefficients, demonstrated that the model structure can accurately predict the fouling behaviour of oil-water mixture at a given operating condition [4]. The models also demonstrated the cake layer accumulation as dominate fouling formation in oil/water separation treatment compared to other foulant formation. In the experimentation studies [81, 82] to validate Hermia laws, the supercritical TMP was applied in both studies without any significant reduction in model accuracy. Several alteration on blockage models have been introduced to account for varying operating parameters such CFV and feed concentration. The CFV was incorporated into block model by introducing the critical flux concept and the feed concentration was incorporated into block by introducing the concentration concept.

4.1.1De Bruijn fouling models

Most fouling models relating permeate flux to time are considered to be exponential shaped on fouling curves[4]. However most of this model are unable to predict blocking phenomena.[22]developed blockage laws based on dead-end filtration.Field et al. [76]modified Hermia's blockage laws by incorporating cross-flow shear rate effect[31]. [83] also developed blockage model by integrating filtration laws and Hermia blockage laws. During De Bruijn modelling process, the following assumptions were made[83].

I. Membrane fouling only depends on permeate flux decline not concentration polarization
II. The membrane structure has composed geometry with regular cylindrical shaped pore radius and length
III. The operating conditions during experimentation are below critical blockage condition, therefore blockage mechanism is negligible

4.1.1.1 Complete blockage

Considering the complete blockage under critical flux alteration, the model equation was derived from the relationship between the permeate flux decline and pore area decrease as shown below[83]:

$$-\frac{1}{J_0}\frac{dJ_{cb}}{dt} = -\frac{1}{a_0}\frac{da_{cb}}{dt} \qquad (5)$$

Whereby (J_0) and (a_0) are initial flux and pore area respectively. The complete blocked pore area (a_{cb}) is defined by product of complete blocked volume (V_{cb}) and shear stress (σ). Whereby the shear stress depends on the physicochemical of solute properties as define in [22, 83]

$$\sigma = \frac{3\rho_{fe} m_s}{2\rho_s d_s \psi} \qquad (6)$$

However, it should be noted that, the shear force in CF filtration can only be effective in removing foulants accumulated on the pore mouth not inside the pore. Also the open pore area is define by De Bruijn et al.[83];

$$a = a_0 - \sigma V_{cb} + \int_0^t \gamma a_0 dt \qquad (7)$$

After integrating and substituting the initial membrane porosity (ε_o) the following corresponding equation is obtained [83]

$$\frac{da}{dt} = -\sigma\frac{a_0}{\varepsilon_0} J_{cb} + \gamma a_0 \qquad (8)$$

After further substitution of equation (6), (7) into Equation (8) the resulting equation (9) is obtained as[83]:

$$\frac{dJ_{cb}}{dt} = -\alpha\left(J_{cb} - J_{cri}\right) \qquad (9)$$

Whereby:

$$J_{cri} = \frac{2\rho_s d_s \psi \varepsilon_0 \gamma}{3\rho_{fe} m_s} \quad \text{and} \quad k_{cb} = \frac{3\rho_{fe} m_s J_0}{2\rho_s d_s \psi \varepsilon_0}$$

4.1.1.2 Summary

The cross flow shear effect has no impact on the standard blockage fouling as it occurs inside the membrane pores. Introduction of critical flux on blockage laws based on both dead-end and cross filtration (excluding standard blockage for CF) has proven to be an effective approach to evaluate fouling behaviour. In membrane filtration, the

International Journal of Emerging Technology and Advanced Engineering
Website: www.ijetae.com (E-ISSN 2250-2459, Scopus Indexed, ISO 9001:2008 Certified Journal, Volume 12, Issue 07, July 2022)

critical flux is a well-defined and observed concept, It generally used for measuring membrane performance [4]. Its measurement criteria depends on operating parameters such as: membrane porosity, solute density, solute forming factor, solute diameter, hydrodynamics, temperature and applied pressure[76].

4.1.2 Kilduff blockage models

Feed concentration has an effect on the fouling behaviour, therefore it should be incorporated in Hermia blockage laws, as it was initially assumed to be a constant parameter in Hermia laws [4]. The following assumption were made in order to take feed concentration in account[4, 70].

I. Membrane geometry and flow rate type were assumed to be regular shaped and Hagen Poiseuile flow respectively.
II. The temperature and crossflow effect on the fouling behaviour were neglected
III. The membrane is initially exposed to pore blockage followed by gradual cake layer formation which prevents further pore blockage.
IV. Lastly, the foulant accumulation on the membrane is directly proportional to feed concentration as shown below[70].

$$\frac{dA_0}{dt} = -\alpha Q_0 C = -\alpha J_0 A_0 C_0 \qquad (10)$$

The model was validated by several experimental studies across multiple feed concentration level without having a significant effect on the model prediction accuracy[4]. However the model assumption still needs to be validated on the oil/water separation, before final conclusions can be made about the model prediction accuracy[4].

4.1.3 Discussion and interpretation

Block models alteration were developed to explain fouling for CF filtration and to integrate concentration into the models. The initial models were developed for dead-end filtration are continually being used in recent studies for PWT.

If extended models could be validated for PW, model accuracy can be enhanced across different levels of concentration, thus reducing the need to re-estimate the model for different levels of concentration.

4.2 Resistance based models

Another modelling approach to evaluate fouling behaviour is resistance based modelling, whereby fouling is considered to be the resistance. The relationship between permeate flux, TMP, viscosity and resistance was described by Darcy's laws as follows [4]:

$$j = \frac{\Delta P}{\mu R_t} \qquad (11)$$

Whereby (R_t) is total resistance described as follows:

$$\boldsymbol{R_t = R_m + R_c + R_b + R_{ir}} \qquad (12)$$

Where (R_m), (R_c), (R_b) are described as initial membrane resistance, cake layer and pore blockage resistance respectively. The irreversible resistance even though neglected in many models is represented by (R_{ir}). The other neglected parameter is osmotic pressure due to dominance of hydrodynamic effect over diffusive effect[4].

4.2.1 Weinser models

Two alterations of the existing model will be considered, namely the particles distributions relative to pore size, as well as adhesion forces between the particles and the surface of the membrane. Both have a major effect on the cake layer and block resistance. Taking a closer look at the pore blocking and cake layer forming processes, their modelling and integration into existing model systems has been illustrated by numerical simulation studies [19]. Cake layer resistance is generally described by the specific resistance and corresponding cake height accumulation as follows[4]:

$$R_c = \hat{R}_c h_c \qquad (13)$$

Whereby the $(\hat{R}_c)$ and (h_c) are expressed as follows[4]

$$\hat{R} = \frac{180(1-\varepsilon_c)^2}{d^2 \varepsilon_c^3} \quad \text{and} \quad \frac{dh_c}{dt} = K_1 j - K_2 h_c \qquad (14)$$

Where (k_1) and (k_2) are forward and backward transport of cake layer formation and removal respectively.

The pore blockage resistance is described by the relationships of gradual decrease in the effective pore radius (r_p) and effective porosity (ε_0) of the membrane, as follows [4]

$$R_m + R_b = \frac{8h_m}{\varepsilon_0 r_p^2} \qquad (15)$$

4.2.2 Fazana et al. exponential models

International Journal of Emerging Technology and Advanced Engineering
Website: www.ijetae.com (E-ISSN 2250-2459, Scopus Indexed, ISO 9001:2008 Certified Journal, Volume 12, Issue 07, July 2022)

[84]first proposed the fouling resistance model and later [85]modified the model. Further alteration were developed by[86] in order to take into account the exponential increase of TMP, especially after the initial stages of operation. Introducing an exponential term on both the cake layer resistance and pore blockage resistance models, the following corresponding mathematical expression was obtained:

$$R_c = \hat{R}h_c\rho_c \cdot e^{n_c t} \qquad (19)$$

$$R_m + R_p = \frac{8h_m}{\varepsilon_0 r_p} \cdot e^{n_b t} \qquad (20)$$

The cake layer density model in equation (19) was also modified to obtain the following expression.

$$\rho_c \frac{dh_c}{dt} = jC - Cjk_4 \qquad (21)$$

4.2.3 Discussion and interpretation of the model

The models are comprehensive and the relationship of the investigated parameters are well defined [4]. However, a few areas are left unidentified by the models. Firstly, the development of the height of the cake is defined to a certain degree of which the exact correlation of CF, concentration, and cake growth remain unknown. Second, there is a lack of a full explanation of how the resistance to pore blockage evolves over time, more specifically how porosity (ε_0) and pore radius (r_p) are developed into the final equation. Thirdly, the initial model accuracy has not been validated against experimental evidence, although the modified version of the model was validate by Giraldo et al.[85]. Also the introduction of the exponential extension resulted to an insignificant improvement of model accuracy in equation(17).

4.2.4 Summary

Between the block laws and resistance based models, resistance models are the most complex and comprehensive type. Therefore block models due to their simplicity, are the commonly used type[4]. Furthermore, despite the unpredictable oil droplet deformation and permeation, blockage models have been used to describe this unpredictable nature of oil droplet permeation on membrane[4]. Also, due to reasonable prediction accuracy by block models under intense operating condition such as supercritical TMP, the blockage models have gained a reputable reputation on oil/water separation application [4].

To date, several alteration on blockage and resistance models have been introduced to account for varying operating parameters such CFV and feed concentration. To identify the impact of CF, the concept of critical flux is integrated into the models. The critical flux is defined as the flux limit where almost no fouling occurs below and a large increase in fouling growth can be observed above it[4]

V. Conclusion

This review involves a detailed investigation into identifying critical operating condition during backwash, permeate flux recovery and membrane fouling models with the objective to develop an improved backwash system, which is considered as the most efficient technique for fouling mitigation. Studies reported in this literature reviews about the optimization of the backwash procedure are varied and depend on the target applications. Numerous backwash models have been developed to improve membrane performance for effective oil/water separation [4]. Most of these developed backwashing system are inefficient, due to poor modelling of relevant physical parameters and variables that affect backwash system [87]. On the contrary, any improvement to the backwashing technique has huge potential to improve the overall filtration performance in membrane technology. The influence of each individual parameters on backwash efficiency has been addressed by several studies in attempt to optimize the backwash procedure.Evaluation of critical parameters by models offers insight into the backwash and fouling action mechanisms. The complexity of filtration and backpulse can reduce by modelling. Modelling helps identify the effect of this parameters (individual and the collective dynamic relationship) on operation conditions.

The reliable model not only can it safe time, but can also reduce cost associated with multiple experiments required to obtain optimal operating condition during backpulse [6]. This modelling approach has proven to yield better understanding of these complex membrane systems. They also help in minimizing the number of experimentation required to validate findings. Since the initial introduction of these modelling techniques, they have been modified to satisfy each target of application[19]. This modelling approach has proven to be a useful tool to help opens new application areas in membrane technology, as it stimulates new ideas for mathematical and physical modelling and algorithms [19].

International Journal of Emerging Technology and Advanced Engineering
Website: www.ijetae.com (E-ISSN 2250-2459, Scopus Indexed, ISO 9001:2008 Certified Journal, Volume 12, Issue 07, July 2022)

VI. Future Scope

Any improvement to the backwashing technique has a huge potential to improve the overall performance, cost-effectiveness of both current and future membrane technology.Although previous studies demonstrate backwash to be an effective approach to mitigate membrane fouling. Backwash cleaning efficiency is highly depended on the following factors: understanding membrane fouling (such as the origin and the precursors of the fouling formation is essential) and the subsequent permeate flux recovery models. Future studies in optimizing membrane backwash system, should address the following:

I. Identifying a model to accurately prediction the permeate flux declines during oil/water separation
II. Identify a model with a reasonable flux recovery prediction accuracy
III. They should also focus onincreasing the intensity backwash procedure, by developing a model with best parameters(pressure, temperature and velocity)that give the best performance during operation.

This study highlights the need to advance understanding and development of membrane backwash process, through models that can evaluate all the important parameters. For example, backwash procedure can be improved by optimizing key parameters, such as: temperature, back-pressure and the corresponding flow velocity. Models provide a useful platform to study the effect of different operating parameters. Lastly, some of the identified models in this review article only require refinements to improve their prediction accuracy and resolution for oil/water separation application.

Acknowledgement

The academic journey, is painful and often much too difficult to bear alone. As such, I would like to acknowledge the following individuals who made it possible for me: Firstlywould like to thank my family for the support. Second, I would like to thank my supervisors Prof. T.B. Tengen, Prof. A.A. Alugongo and Dr.P.B. Sob for their guidance and shared wisdom. Lastly, I would like to thank Vaal University of Technology for the support and knowledge

REFERENCES

[1] T. Ando, k. Akamatsu, S. Nakao, and M. Fujita, "Simulation of fouling and backwash dynamics in dead-end microfiltration: Effect of pore size," Journal of Membrane Science, vol. 392-393, pp. 48-57, 2012.

[2] F. Yalcinkaya, E. Boyraz, J. Maryska, and K. Kucerova, "A Review on Membrane Technology and Chemical Surface Modification for the Oily Wastewater Treatment," Materials, vol. 13, no. 493, pp. 1-14, January 20 2020.

[3] C. A. Scholes, "Pilot plants of membrane technology in industry: Challenges and key learnings," Chem. Sci. Eng., pp. 1-12, November 7 2019.

[4] K. L. Jepsen, M. V. Bram, S. Pedersen, and Z. Yang, "Membrane Fouling for Produced Water Treatment: A Review Study From a Process Control Perspective," Water vol. 10, no. 7, p. 847, 2018.

[5] F. Z. Slimane, F. Ellouze, G. B. Miled, and N. B. Amar, "Physical Backwash Optimization in Membrane Filtration Processes: Seawater Ultrafiltration Case," Journal of Membrane Science and Research, vol. 4, no. 2, pp. 63-68, September 6 2018.

[6] Y. Gao, J. Qin, Z. Wang, and S. W. Østerhus, "Backpulsing technology applied in MF and UF processes for membrane fouling mitigation: A review," Journal of Membrane Science, vol. 587, no. 117136, pp. 1-20, 2019. Elsevier B.V.

[7] Z. Yusuf, N. A. Wahab, and S. Sahlan, "Fouling Control strategy for submerged membrane bioreactor filtration processes using aeration airflow, backwash and relaxation: A review," Desalin. Water Treat., vol. 57, pp. 17683-17695, 2016.

[8] H. Chang et al., "Hydraulic backwashing for low-pressure membranes in drinking water treatment: A review," J.Membr.Sci, vol. 540, pp. 362-380, 2017.

[9] J. C. Lin, D. Lee, and C. Huang, "Membrane Fouling Mitigation: Membrane Cleaning," Separation Science and Technology, vol. 45, no. 7, pp. 858-872, 2010. Taylor & Francis

[10] B. Mi and M. Elimelech, "Organic fouling of forward osmosis membranes: Fouling reversibility and cleaning without chemical reagents," Journal of Membrane Science, vol. 348, pp. 337-345, November 18 2010. Elsevier B.V.

[11] G. Pearce, "Introduction to membranes: Fouling control.," filtr. Sep., vol. 44, pp. 30-32, 2007.

[12] V. G. J. Rodgers and R. E. Sparks, "Reduction of membrane fouling in the ultrafiltration of binary protein mixtures," AIChE J., vol. 37, pp. 1517-1528, 1991.

[13] N. O. Yigit, G. Civelekoglu, I. Harman, H. Koseoglu, and M. Kitis, "Effects of various backwash scenarios on membrane fouling in a membrane bioreactor," Desalination,, vol. 237, pp. 346-356, 2009.

[14] N. Hilal, O. O. Ogunbiyi, N. J. Miles, and R. Nigmatullin, "Methods employed for control of fouling in MF and UF membrane: A comprehensive review," Separation Science and Technology, vol. 40, no. 10, pp. 1957-2005, 2005.

[15] N. Kalboussi, J. Harmand, A. Rapaport, T. Bayen, and N. Ben Amar, "Optimal control of physical backwash strategy - towards the enhancement of membrane filtration process performance," Journal of Membrane Science, vol. 545, no. 9, pp. 38-48, 2017.

[16] P. Srijaroonrat, E. Julien, and Y. Aurelle, "Unstable secondary oil/water emulsion treatment using ultrafiltration: fouling control by backflush," Journal of Membrane Science, vol. 51, no. 2, pp. 11-20, 1999.

[17] S. E. Weschenfelder, A. M. T. Louvisse, C. P. Borges, and J. C. Campos, "Preliminary Studies on the Application of Ceramic

Membranes for Oilfield Produced Water Management," OTC Brasil, 2013: Offshore Technology Conference.

[18] J. Wu, P. Le-Clech, R. M. Stuetz, A. G. Fane, and V. Chen, "Effects of relaxation and backwashing conditions on fouling in membrane bioreactor," Journal of Membrane Science, vol. 324, no. 1-2, pp. 26-32, 2008.

[19] R. Ghidossi, D. Veyret, and P. Moulin, "Computational fluid dynamics applied to membranes: State of the art and opportunities," Chemical Engineering and Processing, vol. 45, pp. 437-454, 2006.

[20] R. Sondhi, Y. S. Lin, and F. Alvarez, "Crossflow filtration of chromium hydroxide suspension by ceramic membrane: fouling and its minimizationby backpulse," J.Membr.Sci, vol. 174, pp. 111-122, 2000.

[21] T. A. Saleh and V. K. Gupta, "Chapter 2 - membrane fouling and strategies for cleaning and fouling control, Nanomaterial and Polymer Membranes: Synthesis, Characterization, and Applications," Elsevier, Amsterdam, pp. 25-53, 2016.

[22] J. Hermia, "Constant pressure blocking filtration law: Application to power-law non-Newtonian fluid," Trans. Inst. Chem. Eng, vol. 60, pp. 183-187, 1982.

[23] W. Guo, H. H. Ngo, and G. Li, " A mini-review on membrane fouling,," Bioresour. Technol, vol. 122, pp. 27-34, 2012.

[24] M. Clifton, N. Abidine, P. Aptel, and V. Sanchez, "Growth of the polarization layer in ultrafiltration with hollow-fibre membranes," J. Membr. Sci., vol. 21, pp. 233-245, 1984.

[25] P. J. Smith, S. Vigneswaran, H. H. Ngo, R. Ben-Aim, and H. Nguyen, "A new approach to backwash initiation in membrane systems," Journal of Membrane Science, vol. 278, pp. 381-389, 2006.

[26] V. Kuberkar, P. Czekaj, and R. Davis, "Flux enhancement for membrane filtration of bacterial suspensions using high-frequency backpulsing," Biotechnol. Bioeng, vol. 60, pp. 77-87, 1998.

[27] H. M. Ma, D. R. Nielsen, C. N. Bowman, and R. H. Davis, "Membrane surface modification and backpulsing for wastewater treatment," Separ. Sci. Technol, vol. 36, pp. 1557-1573, 2001.

[28] Y. Wei, H. Qi, X. Gong, and S. Zhao, "Specially Wettable Membrane for Oil-Water Separation-Review," Adv. Mater. Interfaces, vol. 5, no. 1800576, p. 27, 2018.

[29] C. Causserand, D. Pellegrin, and J. C. Rouch, "Effects of sodium hypochlorite exposure mode on PES/PVP ultrafiltration membrane degradation," Water Res., vol. 85, pp. 316-326, 2015.

[30] S. Huang, R. A. Ras, and X. Tian, "Antifouling membranes for oily wastewater treatment: Interplay between wetting and membrane fouling," Current Opinion in Colloid & Interface Science, vol. 36, pp. 90-109, February 15 2018. Elsevier B.V.

[31] M. Padaki et al., "Membrane technology enhancement oil-water separation," Desalination, vol. 357, pp. 197-207, 2015.

[32] Y. Peng, F. Guo, Q. Wen, F. Yang, and Z. Guo, "A novel polyacrylonitrile membrane with a high flux for emulsified oil/water separation," in Separation and purification TechnologyWuhan: ELSEVIER B.V, 2017, pp. 72-78.

[33] S. H. Silalahi, "Treatment of Produced Water: Development of Methods and Discharge," Norwegian University of Science and Technology, Trondheim2010.

[34] H. Krawczyk and A. S. Jonsson, "Separation of dispersed substances and galactogluco-mannanmannan in thermomechanical pulp process water by microfiltration," Separ. Purif. Technol., vol. 79, pp. 43-49, 2011.

[35] B. L. McAlexander and D. W. Johnson, "Backpulsing fouling control with membrane recovery of light non-aqueous phase liquids," J. Membr. Sci, vol. 227, pp. 137-158, 2003.

[36] W. D. Mores, C. N. Bowman, and R. Davis, "Theoretical and experimental flux maximization by optimization of backpulsing,," J. Membr. Sci., vol. 165, pp. 225-236, 2000.

[37] G. Green and G. Belfort, "fouling of Ultrafiltrationmembrane lateral migation and the particle trajectory model," Desalination, vol. 35, pp. 129-147, 1980.

[38] D. A. Drew, J. A. Schonberg, and G. Belfort, "Lateral intertial migration of a small sphere in fast laminar flow through a membrane duct," Chemical Engineering Science, vol. 46, pp. 3219-3224, 1991.

[39] S. Ripperger and J. Altamann, "Crossflow microfiltration- state of art, ." Separ.Purif. Technol, vol. 26, pp. 25-36, 2002.

[40] T. Darvishzadeh and N. V. Priezjev, "Effects of crossflow velocity and transmembrane pressure on microfiltration of oil-in-water emulsions.," Journal Membrane Science, vol. 423-424, pp. 468-476, 2012.

[41] T. Darvishzadeh, V. T. Tarabara, and N. V. Priezjev, "Oil droplet behavior at a pore entrance in presence of crossflow: Implication for microfiltration of oil-water dispersions," physics.flu-dyn, vol. 1, pp. 1-37, 2018.

[42] T. Darvishzadeh, B. Bhattarai, and N. V. Priezjev, "The Critical Pressure for Microfifiltration of Oil-in-Water Emulsions Using Slotted-Pore Membranes," Journal of Membrane Science, vol. 563, no. 412, pp. 610-616, 2018.

[43] E. N. Tummons, V. V. Tarabara, J. W. Chew, and A. G. Fane, "Behavior of oil droplet at the membrane surface during crossflow microfiltration of oil-water emulsions," Journal of Membrane Science vol. 500, pp. 211-224, 2016.

[44] Nazzal and M. R. Wiesner, "Microfiltration of oil-in-water emulsions," Water Environ.Res, vol. 68, pp. 1187-1191, 1996.

[45] Fluent, "Fluent 6.1 Users Guide," FLUENT 6.12003.

[46] B. D. Nicoles and C. W. Hirt, "Volumeof Fluid (VOF) method for the dynamics of free boundaries," J.Comput.Phys, vol. 201, p. 39, 1981.

[47] T. Darvishzadeh, V. V. Tarabara, and N. V. Priezjev, "Oil droplet behavior at a pore entrance in the presence of crossflow: Implication for microfiltration of oil/water despersion," Journal Membr.Sci, vol. 442, p. 447, 2013.

[48] F. L. Hua, F. Tsang, F. J. Wang, S. Y. Chan, H. Chua, and S. N. Sin, "Performance study of ceramic microfiltration membrane for oily wastewater treatment," Chem.Eng.J, vol. 128, pp. 169-175, 2007.

[49] S. Ashaghi, M. Ebrahimi, and P. Czermak, "Ceramic Ultra- and Nanofiltration Membranes for Oilfield Produced Water Treatment: A Mini Review," Open Environmental Science, vol. 1, pp. 1-8, 2007.

[50] K. T. Tompkins, L. P. Murphy, B. L. Owsenek, R. P. Pignataro, and A. T. Rodriguez, "Ultrafiltration Membrane polishing system for shipbord Treatment of oily wastwater. ," Naval Sea systems Command (SEA03R16) Crystal City, VA 22242,2007, Accessed on: October/05/2020.

[51] S. R. H. Abadi, M. R. Sebzari, M. Hemati, F. Rekabdar, and T. Mohammadi, "Ceramic membrane performance in microfiltration of oily wastewater," Desalination, vol. 265, no. 1, pp. 222-228, 2011.

[52] A. L. Ahmad, S. Ismail, and S. Bhatia, "Ultrafiltration behavior in the treatment of agro-industry effluent: pilot scale studies," Chemical Engineering Science, vol. 60, pp. 5385-5394, 2005.

[53] S. Lee, U. Aurelle, and H. Roques, "Concentration polarization, membrane fouling and cleaning in ultrafiltration of soluble oil,," Journal of membrane Science, vol. 19, pp. 23-38, 1984.

[54] F. L. Hua, Y. F. Tsang, Y. J. Wang, S. Y. Chan, H. Chua, and S. N. Sin, "Performance study of ceramic microfiltration membrane for oily wastewater treatment," Chemical Engineering Journal, vol. 128, pp. 169-175, 2007.

[55] P. Mikulasek, P. Dolecek, D. Smidova, and P. Pospisil, "Cross flow microfiltration of mineral dispersions using ceramic membranes," Desalination, vol. 163, pp. 333-343, 2004.

[56] A. Salahi, T. Mohammadi, A. Rahmat Pour, and F. Rekabdar, "Oily wastewater treatment using ultrafiltration,," Desalination and Water Treatment, vol. 6, pp. 289-298, 2009.

[57] T. Mohmmadi, M. Kazemimoghadam, and M. Saadabadi, "Modeling of membrane fouling and decline in reverse osmosis during separation of oil in water emulsions," Desalination, vol. 157, pp. 369-375, 2003.

[58] S. Redkar, V. Kuberkar, and R. H. Davis, "Modeling of concentration polarization and depolarization with high-frequency backpulsing," J. Membr. Sci., vol. 121, pp. 229-242, 1996.

[59] C. A. Romero and R. H. Davis, "Experimental verification of the shear-induced hydrodynamic diffusion model of crossflow microfiltration," J. Membr. Sci., vol. 62, pp. 249-273, 1991.

[60] L. J. Zeman and A. L. Zydney, "Bulk mass transport, Microfiltration and Ultrafiltration Principles and Application," New York, 1996: Mercel Dekker.

[61] J. Cakl and P. Doleèek, "Boundary layer phenomena in backflushed cross-flow microfiltration," Prague, 1998: 13th International CHISA Congress,.

[62] J. Murkes and C. G. Carlsson, Crossflow Filtration: Theory and Practice. Chichester: Wiley, 1988.

[63] R. Liikanen, J. Yli-Kuivila, and R. Laukkanen, "Efficiency of various chemical cleanings for nanofiltration membrane fouled by conventionally-treated surface water," J. Membr. Sci., vol. 195, pp. 265-276, 2002.

[64] M. Zator, J. Warczok, M. Ferrando, F. Lo´ pez, and C. Gu¨ ell, "Chemical cleaning of polycarbonate membranes fouled by BSA/dextran mixtures," J. Membr. Sci., vol. 327, pp. 59-68, 2009.

[65] S. Chellam, J. G. Jacangelo, and T. P. Bonacquisti, "Modeling and experimental verification of pilot-scale hollow fiber, direct flow microfiltration with periodic backwashing.," Environ. Sci. Technol., vol. 32, pp. 75-81, 1998.

[66] S. S. Madaeni and Y. Mansourpanah, "Chemical cleaning of reverse osmosis membranes fouled by whey.," Desalination, vol. 161, pp. 13-24, 2004.

[67] D. Wu and M. R. Bird, "The fouling and cleaning of ultrafiltration membranes during the filtration of model tea component solutions.," J.Food Process Eng., vol. 30, pp. 293–323, 2007.

[68] Z. Wu, C. Zhang, K. Peng, Q. Wang, and Z. Wang, "Membrane fabrication for oil/water separtion," Environ. Sci. Eng., vol. 12, no. 3, p. 15, April 27 2018.

[69] A. Salahi, M. Abbasi, and T. Mohammadi, "Permeate flux decline during UF of oily wastewater: Experimental and modeling.," Desalination, vol. 251, pp. 153-160, 2010.

[70] C. Duclos-Orsello, W. Li, and C. C. C. Ho, "A three mechanism model to describe fouling of microfiltration membranes," J. Membr. Sci., vol. 280, pp. 856-866, 2006.

[71] A. Lobo, M. Benito, and C. Pazos, "Ultrafiltration of oil-in-water emulsions with ceramic membranes: Influence of pH and crossflow velocity," J. Membr. Sci., vol. 278, pp. 328-334, 2006.

[72] P. Pedenaud, S. Heng, W. Evans, and D. Bigeonneau, "Ceramic membrane and core pilot results for produced water management. ," in In Proceedings of the Annual Offshore Technology Conference, Rio de Janeiro, Brazil, 2011, pp. 385–400.

[73] R. Badrnezhad and A. H. Beni, "Ultrafiltration membrane process for produced water treatment: Experimental and modeling.," J. Water Reuse Desalin., vol. 3, p. 249, 2013.

[74] J. Busch, A. Cruse, and W. Marquardt, "Modeling submerged hollow-fiber membrane filtration for wastewater treatment.," J. Membr. Sci., vol. 288, pp. 94–111, 2007.

[75] A. N. L. Ng and A. S. Kim, "A mini-review of modeling studies on membrane bioreactor (MBR) treatment for municipal wastewaters.," Desalination, vol. 212, pp. 261–281, 2007.

[76] R. W. Field, J. Wu, J. A. Howell, and B. B. Gupta, "Critical flux concept for microfiltration fouling," J. Membr. Sci., vol. 100, pp. 259–272., 1995,.

[77] A. Maiti, M. Sadrezadeh, S. Guha Thakurta, D. J. Pernitsky, and S. Bhattacharjee, "Characterization of boiler blowdown water from steam-assisted gravity drainage and silica-organic coprecipitation during acidification and ultrafiltration," Energy Fuels, vol. 26, pp. 5604–5612., 2012.

[78] M. Ebrahimi et al., "Characterization and application of different ceramic membranes for the oil-field produced water treatment," Desalination, vol. 245, pp. 533–540., 2009.

[79] B. Chakrabarty, A. K.Ghoshal, and M. K. Purkait, "Cross-flow ultrafiltration of stable oil-in-water emulsion using polysulfone membranes," Chem. Eng. J., vol. 165, pp. 447–456, 2010.

[80] M. C. Vincent Vela, S. Álvarez Blanco, J. Lora García, and E. Bergantiños Rodríguez, "Analysis of membrane pore blocking models adapted to crossflow ultrafiltration in the ultrafiltration of PEG.," Chem. Eng. J., vol. 149, pp. 232–241, 2009.

[81] H. Peng and A. Y. Tremblay, "Membrane regeneration and filtration modeling in treating oily wastewaters.," J. Membr. Sci., vol. 324, pp. 59–66, 2008.

[82] A. Salahi, M. Abbasi, and T. Mohammadi, "Permeate flux decline during UF of oily wastewater: Experimental and modeling," Desalination, vol. 251, pp. 153–160., 2010.

[83] J. P. F. De Bruijn, F. N. Salazar, and R. Borquez, "Membrane blocking in Ultrafiltration A New Approach to Fouling," Trans IChemE., vol. 83, pp. 211-219, 2005.

[84] J. Mallevialle, P. E. Odendaal, and M. R. Wiesner, Water Treatment Membrane Processes. New York: McGraw-Hil, 1996.

[85] E. Giraldo, N. Systems, L. A. Water, and E. Giraldo, "Dynamic Mathematical Modeling of Membrane Fouling in Submerged Membrane Bioreactors," Proc. Water Environ. Fed, vol. 2006, pp. 4895–4913, 2006,.

[86] M. Fazana et al., "Bioresource Technology New and practical mathematical model of membrane fouling in an aerobic submerge," Bioresour. Technol., vol. 238, pp. 86–94, 2017.

[87] A. U. Krupp, I. M. Griffiths, and C. P. Please, "Stochastic modelling of membrane filtration process," Royal Society, vol. 473, p. 17, 2017.